COLUMBIA UNIVERSITY
IN THE CITY OF NEW YORK

JET Collaboration

pQCD energy loss and flavor dependence in CUJET v2.0 & v3.0

Jiechen Xu
Columbia University

Based on: JX, Jinfeng Liao, Miklos Gyulassy, arXiv:1411:3673
JX, Alessandro Buzzatti, Miklos Gyulassy, JHEP 1408, 063 (2014)

For SGW2014, December 9-12, 2014 @ Padova, Italy

Outline

- CUJET -- A pQCD Model for Jet Flavor Tomography at RHIC and LHC
  - Motivations: the "heavy quark puzzle" and the "surprising transparency of QGP at LHC"
  - CUJET2.0 = Dynamical Running Coupling (D)GLV + Elastic Energy Loss + (2+1)D Viscous Hydro
    - Intersection between light hadron and open heavy flavor R_{AA}
- The "high p_T v_2 puzzle"
  - Constrain jet energy loss models: (R_{AA} & v_2) @ (RHIC & LHC)
  - CUJET3.0 = CUJET2.0 + semi-QGP + Magnetic Monopoles
    - *Simultaneously* describe light hadron and open heavy flavor's R_{AA} and v_2 at both RHIC and LHC
- Summary

Jet Tomography in nuclear collisions

- Hard processes happen before the formation of the medium
  - Initial hard parton production rate in AA collisions can be calculated in pQCD
- Quarks and gluons have final state interaction
  - Jets will be modified by interacting with the medium

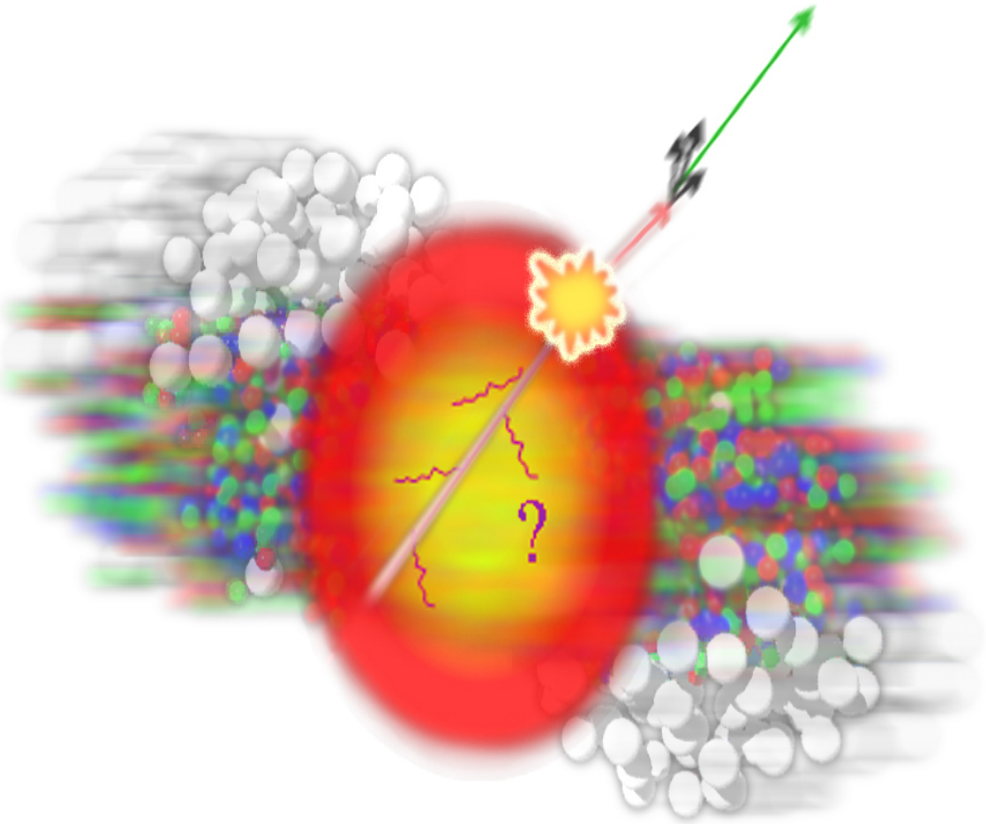

Jet-medium interaction: radiative energy loss

- pQCD jet energy loss models: AMY, ASW, BDMPS-Z, Higher twist, GLV…
- GLV
  - The plasma: static scattering centers
  - Energy loss: expansion in the number of parton-medium scatterings (opacity expansion)
    - Dominated by the first hard contribution. (“Thin plasma”)
  - Include interference of “vacuum” radiation, vertex radiation and gluon rescatterings

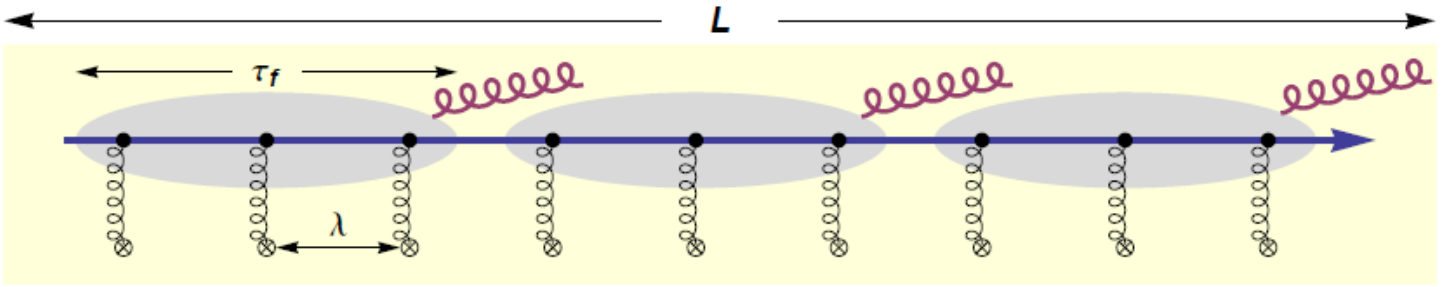

- $\tau_f<\lambda<L$ Incoherent multiple collisions
- $\lambda<\tau_f<L$ LPM effect
- $\lambda<L<\tau_f$ “Factorization” limit

(D)GLV Opacity Expansion

$$x\frac{dN_g^n}{dxd^2\mathbf{k}} = \frac{C_R\alpha_s}{\pi^2}\frac{1}{n!}\left(\frac{L}{\lambda_g}\right)^n \int\prod_{i=1}^{n}\left(d^2\mathbf{q}_i\left(|\bar{v}_i(\mathbf{q}_i)|^2-\delta^2(\mathbf{q}_i)\right)\right)$$

$$\times\ -2\,\mathbf{C}_{(1\cdots n)}\cdot\sum_{m=1}^{n}\mathbf{B}_{(m+1\cdots n)(m\cdots n)}$$

$$\times\left(\cos\left(\sum_{k=2}^{m}\Omega_{(k\cdots n)}\Delta z_k\right)-\cos\left(\sum_{k=1}^{m}\Omega_{(k\cdots n)}\Delta z_k\right)\right)$$

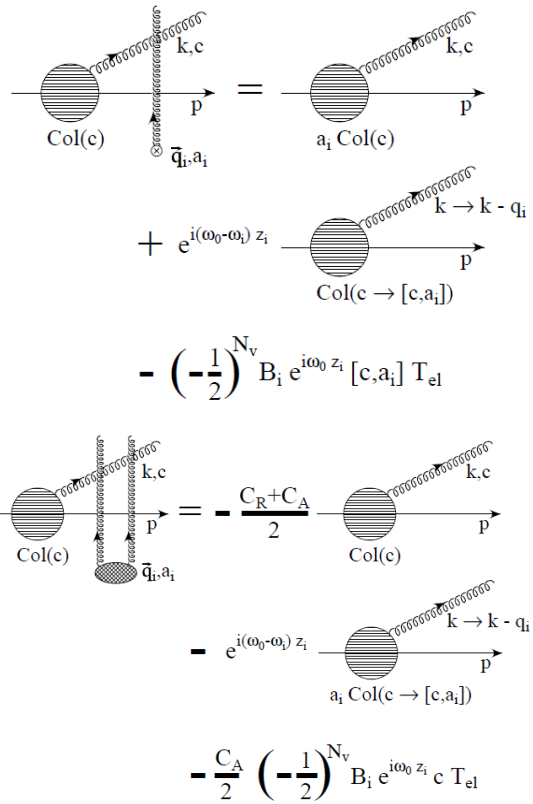

$$\mathbf{C}_{(1\cdots n)} = \frac{\mathbf{k}-\mathbf{q}_1-\cdots-\mathbf{q}_n}{(\mathbf{k}-\mathbf{q}_1-\cdots-\mathbf{q}_n)^2+\chi^2}$$

$$\mathbf{H} = \frac{\mathbf{k}}{\mathbf{k}^2+\chi^2}$$

$$\mathbf{B}_{(i)} = \mathbf{H}-\mathbf{C}_{(i)}$$

$$\mathbf{B}_{(1\cdots m)(1\cdots n)} = \mathbf{C}_{(1\cdots m)}-\mathbf{C}_{(1\cdots n)}$$

$$\Omega_{m\cdots n} = \frac{(\mathbf{k}-\mathbf{q}_m-\cdots-\mathbf{q}_n)^2+\chi^2}{2xE}$$

(Gyulassy, Levai, Vitev, Djordjevic)

$$\chi^2 = M^2x^2 + m_g^2(1-x) \quad m_g = \mu/\sqrt{2}\ ,\ \mu = gT\sqrt{N_c/3+N_f/6}$$

$$|\bar{v}_i(\mathbf{q}_i)|^2 = \frac{{\mu_i}^2}{\pi(\mathbf{q}_i^2+{\mu_i}^2)^2}$$ (Gyulassy-Wang, 1996)

Heavy quark puzzle & Surprising transparency

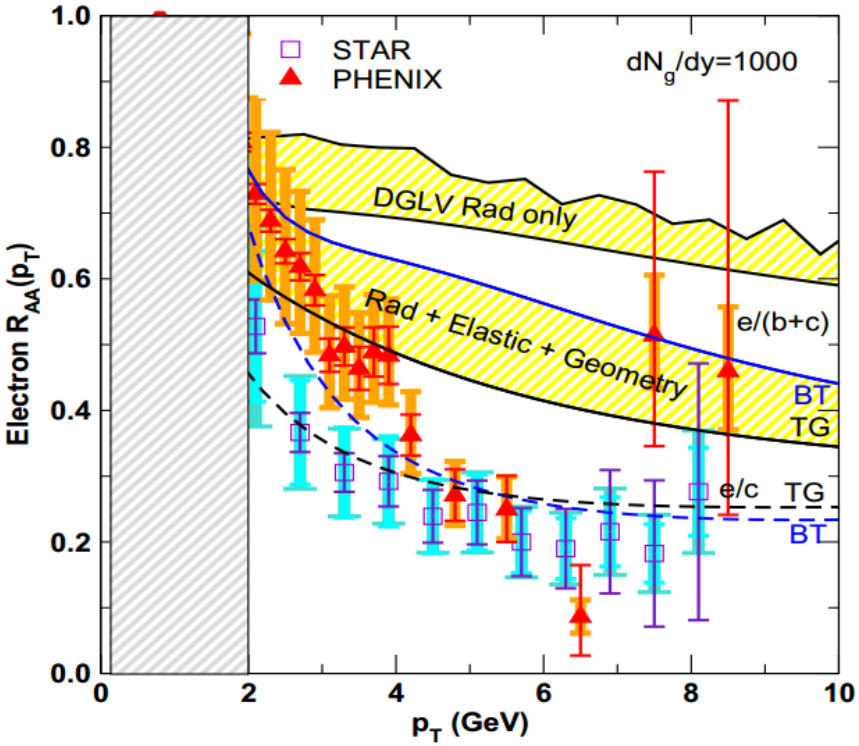

WHDG, NPA784,426(2007)

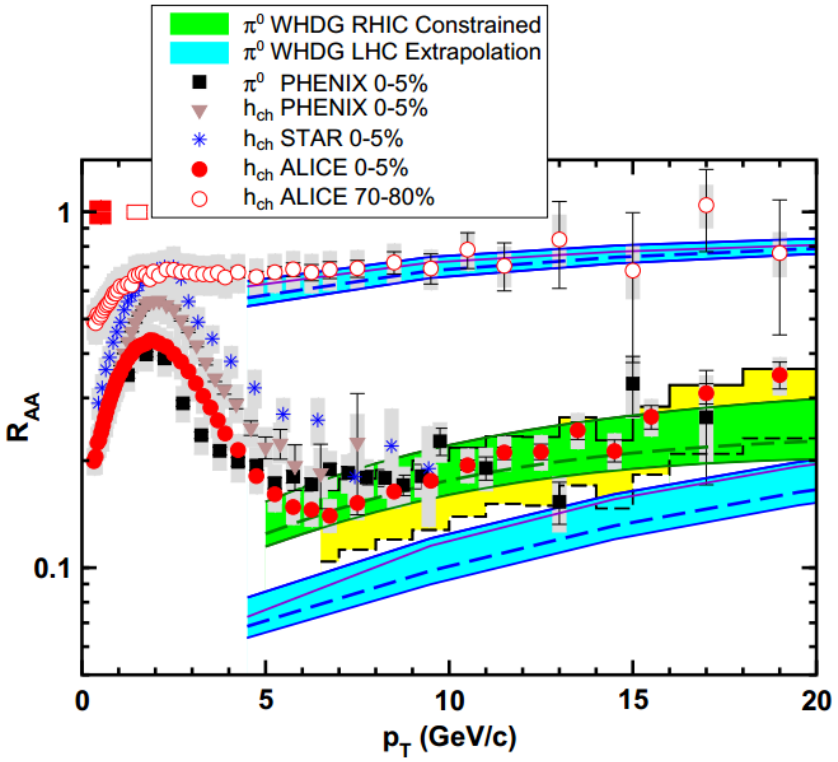

Horowitz and Gyulassy, NPA872,265(2011)

- "Heavy Quark Puzzle"
  - Scattering centers recoil?
  - Different path length fluctuations?
- "Surprising Transparency"
  - The opacity's dependence on density is weaker than linear
  - Smaller coupling at LHC?

CUJET: a solution to heavy quark puzzle

Radiative: dynamical DGLV

$$|\tilde{v}(\mathbf{q},\mathbf{z})|^2 = \frac{f_E^2 - f_M^2}{(\mathbf{q}^2 + f_E^2\mu^2(\mathbf{z}))(\mathbf{q}^2 + f_M^2\mu^2(\mathbf{z}))}$$

$$\lambda_{\rm dyn} \Longleftrightarrow \lambda_{\rm stat} = \frac{\lambda_{\rm dyn}}{c(n_f)}$$

$$\left[\frac{\mu^2}{\boldsymbol{q}^2(\boldsymbol{q}^2+\mu^2)}\right]_{\rm dyn} \Longleftrightarrow \left[\frac{\mu^2}{(\boldsymbol{q}^2+\mu^2)^2}\right]_{\rm stat}$$

Djordjevic and Heinz, PRC (2008)

Elastic: Thoma-Gyulassy (TG)

$$\frac{dE(\mathbf{z})}{d\tau} = -C_R\pi\alpha_s^2 T(\mathbf{z})^2\left(1+\frac{n_f}{6}\right)\log\left(\frac{4T(\mathbf{z})\sqrt{E(\mathbf{z})^2-M^2}}{\left(E(\mathbf{z})-\sqrt{E(\mathbf{z})^2-M^2}+4T(\mathbf{z})\right)\mu(\mathbf{z})}\right)$$

Geometry: path length fluctuations

$$x_E\frac{dN_g^{n=1}}{dx_E}(\mathbf{x}_0,\phi) = \frac{18C_R\alpha_s}{\pi^2}\frac{4+n_f}{16+9n_f}\int d\tau\,\rho(\mathbf{z})\int d^2\mathbf{k}\int d^2\mathbf{q}\;\alpha_s^2|\tilde{v}(\mathbf{q},\mathbf{z})|^2$$
$$\times\;\frac{-2(\mathbf{k}-\mathbf{q})}{(\mathbf{k}-\mathbf{q})^2+\chi^2(\mathbf{z})}\left(\frac{\mathbf{k}}{\mathbf{k}^2+\chi^2(\mathbf{z})}-\frac{(\mathbf{k}-\mathbf{q})}{(\mathbf{k}-\mathbf{q})^2+\chi^2(\mathbf{z})}\right)$$
$$\times\left(1-\cos\left(\frac{(\mathbf{k}-\mathbf{q})^2+\chi^2(\mathbf{z})}{2x_+E}\tau\right)\right)$$
$$\times\left(\frac{x_E}{x_+}\right)J(x_+(x_E))$$

$T(\tau_{max})$=Tf

$$L(\vec{x}_\perp,\phi) = \int d\tau\rho_p(\vec{x}_\perp+\tau\hat{n}(\phi))/\langle\rho_p\rangle$$

WHDG, NPA (2007)

CUJET: a running coupling explanation to the surprising transparency

- Introduce one-loop running strong coupling

$$\alpha_s \longrightarrow \alpha_s(Q^2) = \begin{cases} \alpha_0 & \text{if } Q \le Q_0 \\ \dfrac{2\,\pi}{9\,\log(Q/\Lambda_{QCD})} & \text{if } Q > Q_0 \end{cases}$$

B. G. Zakharov, JETP Lett. 88 (2008) 781-786

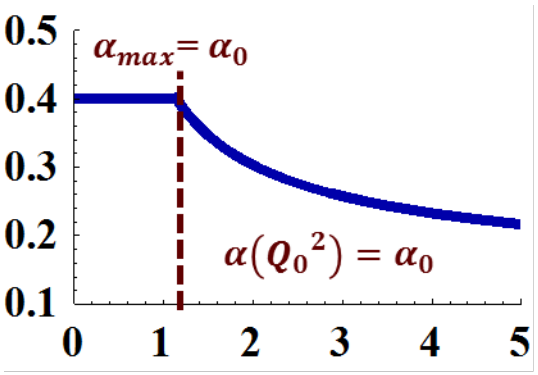

- Multi-scale running strong coupling

$$Q^2 = \mathbf{q}^2$$

$$Q_2^2 = q^2 - M^2 = \frac{\mathbf{k}^2}{x_+(1-x_+)} + \cancel{\frac{x_+ M^2}{1-x_+}} + \cancel{\frac{m_g^2}{x_+}}$$

$$Q^2 = (2T)^2$$

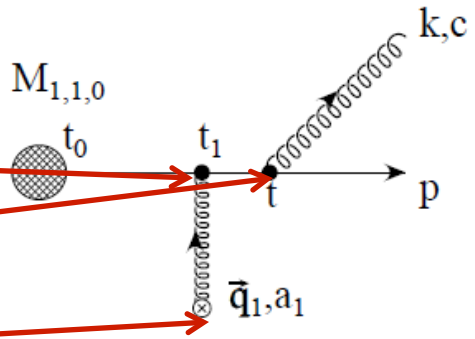

- Elastic:

$$\alpha_s^2 \log\frac{4ET}{\mu^2} \longrightarrow \alpha_s(\mu^2)\alpha_s(4ET)\log\frac{4ET}{\mu^2(\alpha_s(4T^2);T)}$$

S. Peigne and A. Peshier, PRD 77, 114017 (2008)

CUJET2.0: Couple DGLV to 2+1D Viscous Hydro

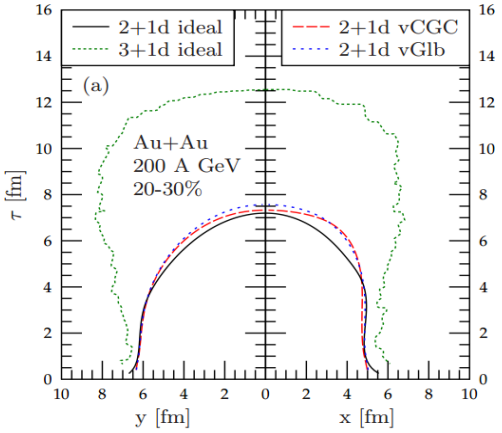

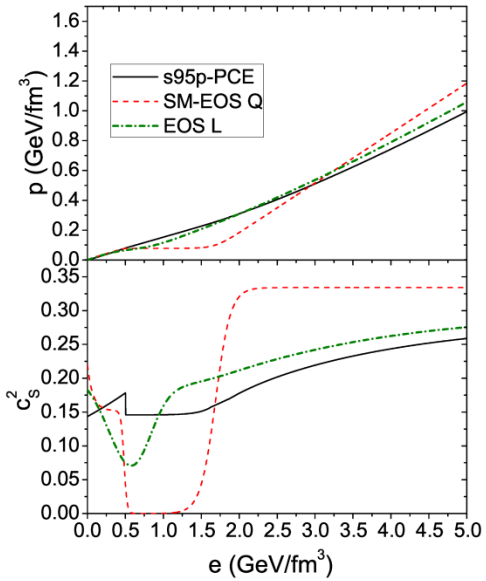

- Couple rcDGLV to VISH2+1 transversely expanding QGP fluid fields (T(x,t),v(x,t))
- RHIC Au+Au 200AGeV & LHC Pb+Pb 2.76ATeV
  - Equaiton of State: s95p-v0-PCE
  - Initial Condition: MC-Glauber
  - η/s=0.08
  - Initial Time: 0.6fm/c
  - Cooper-Frye freeze-out temperature: 120MeV
- Compatible with measurements of low pT particle production spectra and flow harmonics

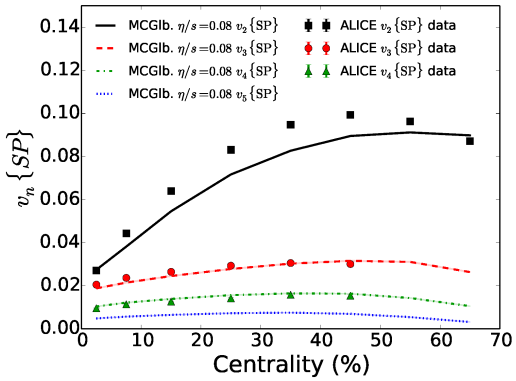

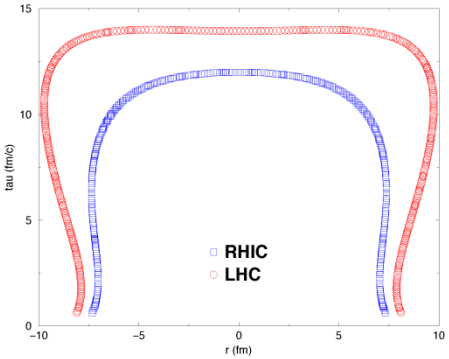

T. Renk, H. Holopainen, U. Heinz and C. Shen, PRC 83, 014910 (2011)
C. Shen, U. Heinz, P. Huovinen and H. Song, PRC 82, 054904 (2010)
H. Song and U. Heinz, PRC 78, 024902 (2008)

Courtesy of Chun Shen

CUJET2.0: π^0 & $h^\pm$ R_{AA} vs p_T

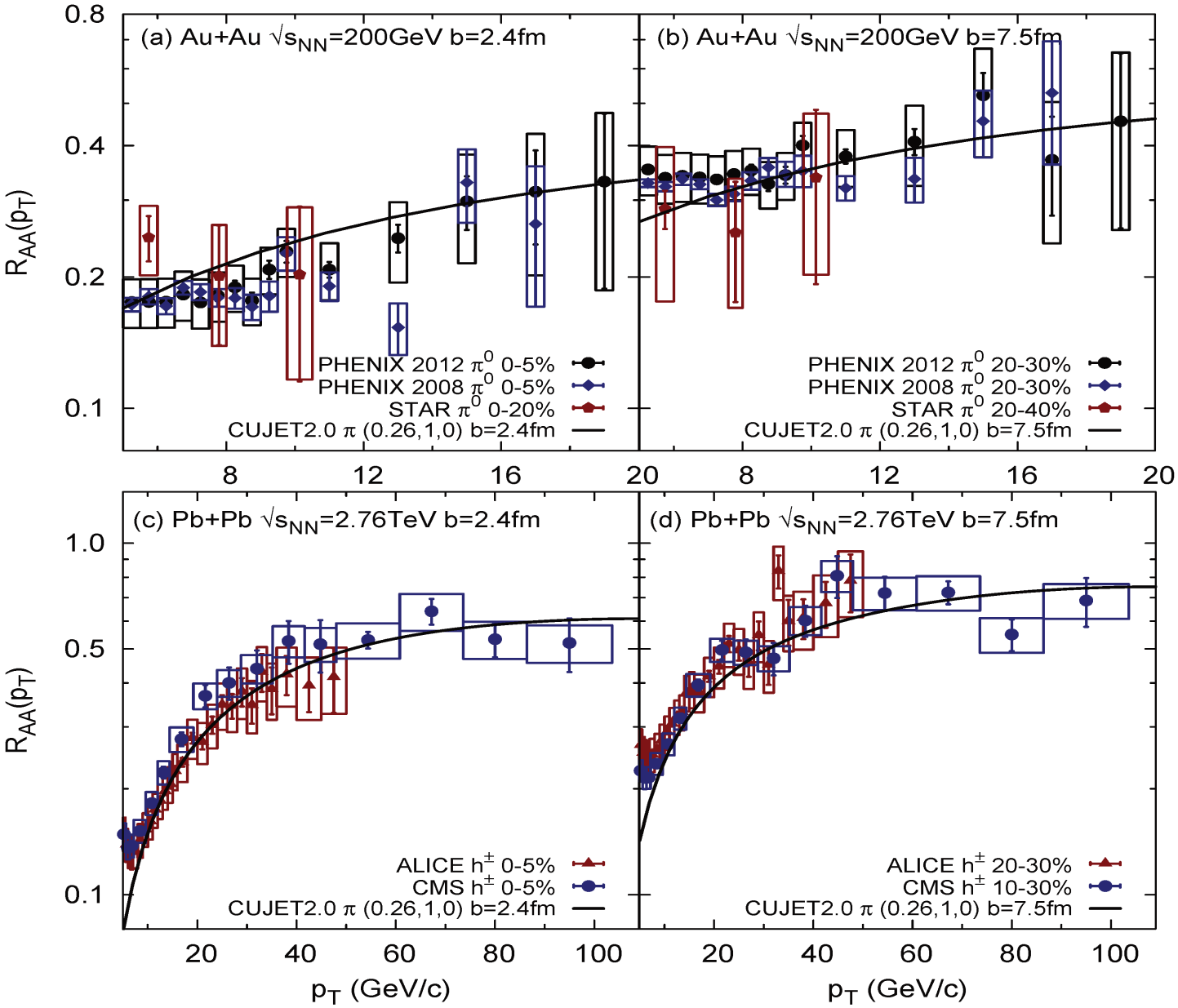

JX, A. Buzzatti, M. Gyualssy, JHEP 1408, 063 (2014)

CUJET2.0: Jet Transport Coefficient

$$\hat{q}(E,T;\alpha_{max},f_E,f_M)=\rho(T)\int_0^{6ET} d\mathbf{q}^2\mathbf{q}^2\frac{d\sigma_{\rm eff}}{d\mathbf{q}^2}$$

$$\frac{d\sigma_{\rm eff}}{d\mathbf{q}^2}=\frac{4\pi C(f_E^2-f_M^2)\alpha_{\rm s}^2(\mathbf{q}^2)}{(\mathbf{q}^2+f_E^2\mu^2(T))(\mathbf{q}^2+f_M^2\mu^2(T))}$$

$$\mu(T)=T\sqrt{4\pi\alpha_s(4T^2)(1+n_f/6)}$$

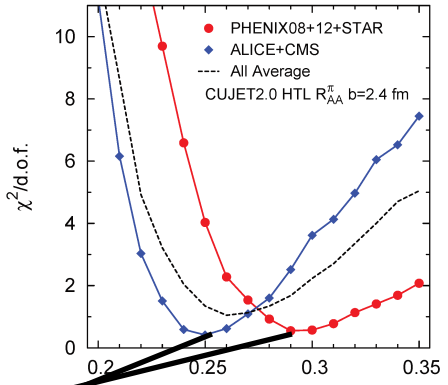

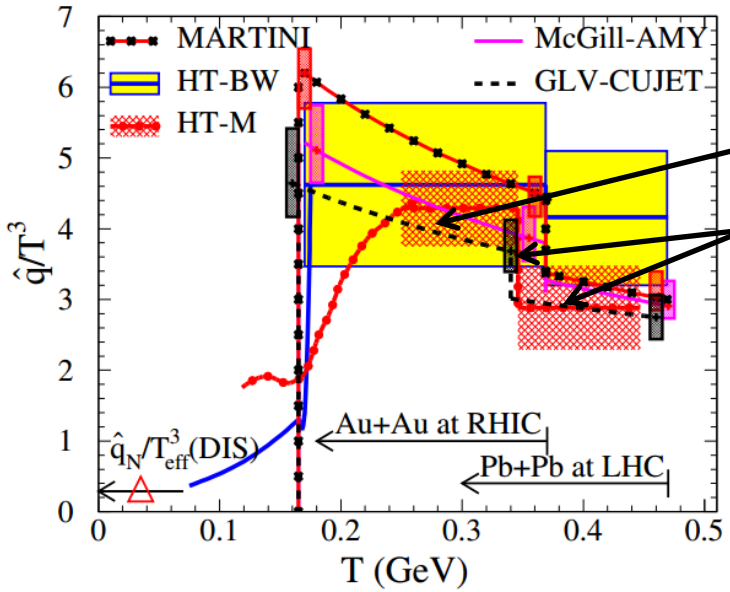

JET Collaboration, PRC 90, 014909 (2014)

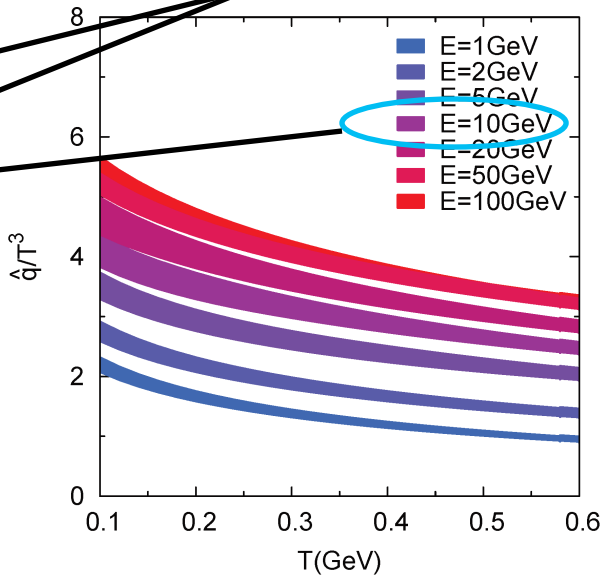

JX, Buzzatti, Gyualssy, JHEP 1408, 063 (2014)

$$\frac{\hat{q}}{T^3}\approx\begin{cases}4.6\pm1.2 & \text{at RHIC,}\\ 3.7\pm1.4 & \text{at LHC,}\end{cases}\qquad \hat{q}\approx\begin{cases}1.2\pm0.3\\ 1.9\pm0.7\end{cases}\ \text{GeV}^2/\text{fm at}\ \begin{matrix}T=370\ \text{MeV},\\ T=470\ \text{MeV},\end{matrix}$$

CUJET2.0: open heavy flavor R_{AA}

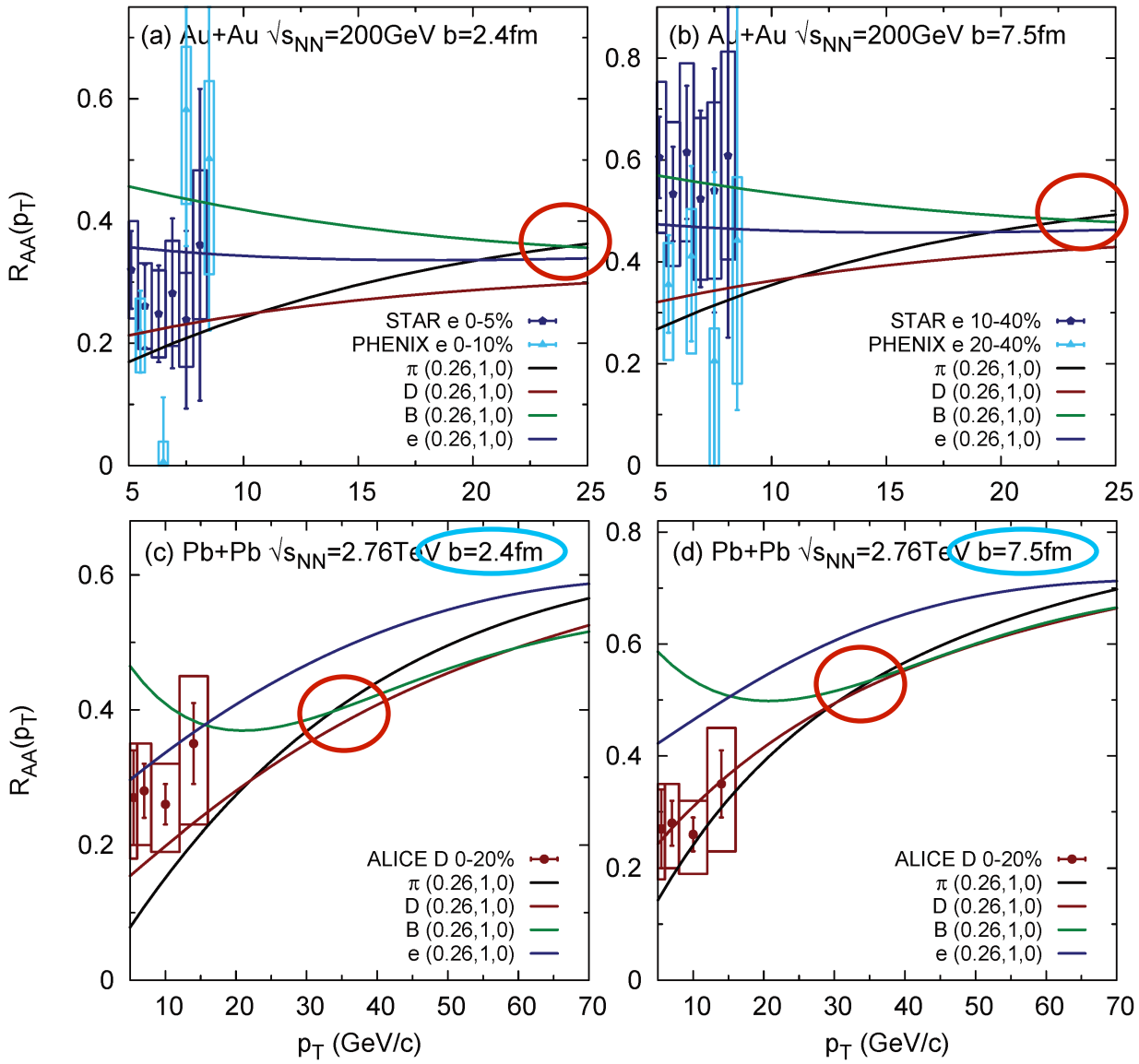

JX, Buzzatti, Gyualssy, JHEP 1408, 063 (2014)

- CUJET2.0 solved "Heavy Quark Puzzle"
  - Dynamical scattering centers
  - Realistic path length fluctuations
  - pQCD production spectra: LO pQCD (g,q) and FONLL (c,b)
- R_{AA} of B meson and $\pi^0/h^{\pm}$ intersect at both RHIC (p_T~25GeV) and LHC (p_T~35GeV), this crossing is almost independent of centrality
- At low pT, D meson and $\pi^0/h^{\pm}$ mixed together, B meson is clearly above them

Why $\pi^0/h^{\pm}$ and beauty R_{AA} have a level crossing?

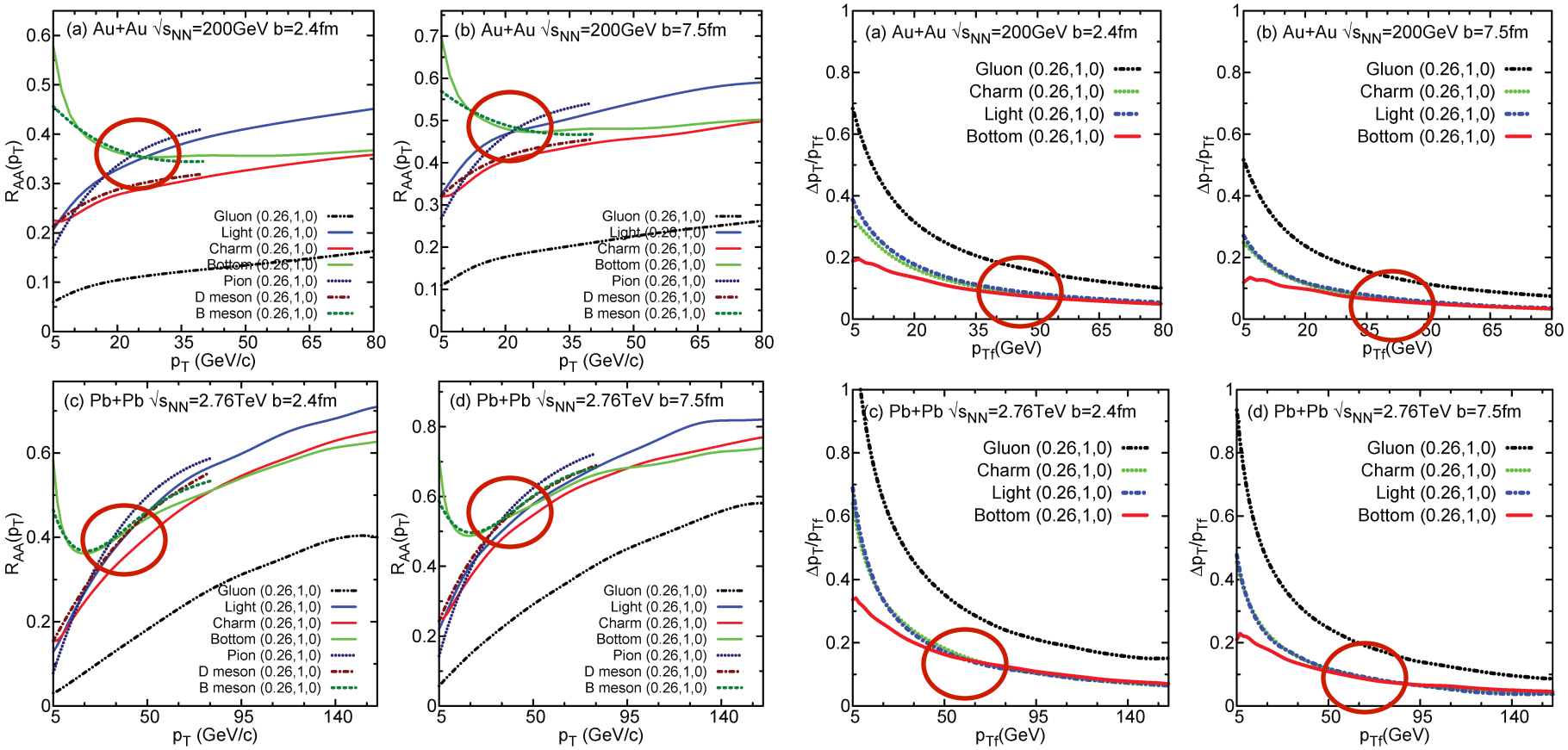

$$\frac{d\bar{\sigma}^{AA\to h}}{d^3p_f} \equiv \frac{1}{N_{bin}}\frac{d\sigma^{AA\to h}}{d^3p_f} = \frac{d\sigma^{pp\to q}}{d^3p_i} \otimes P(E_i(p_i) \to E_f(p_f)) \otimes D(q \to h)$$

- The pp spectrum and partonic energy loss theory combine to induce the level crossing, and the former plays a more critical role

Constrain jet energy loss models: (RHIC + LHC) & (RAA + v2)

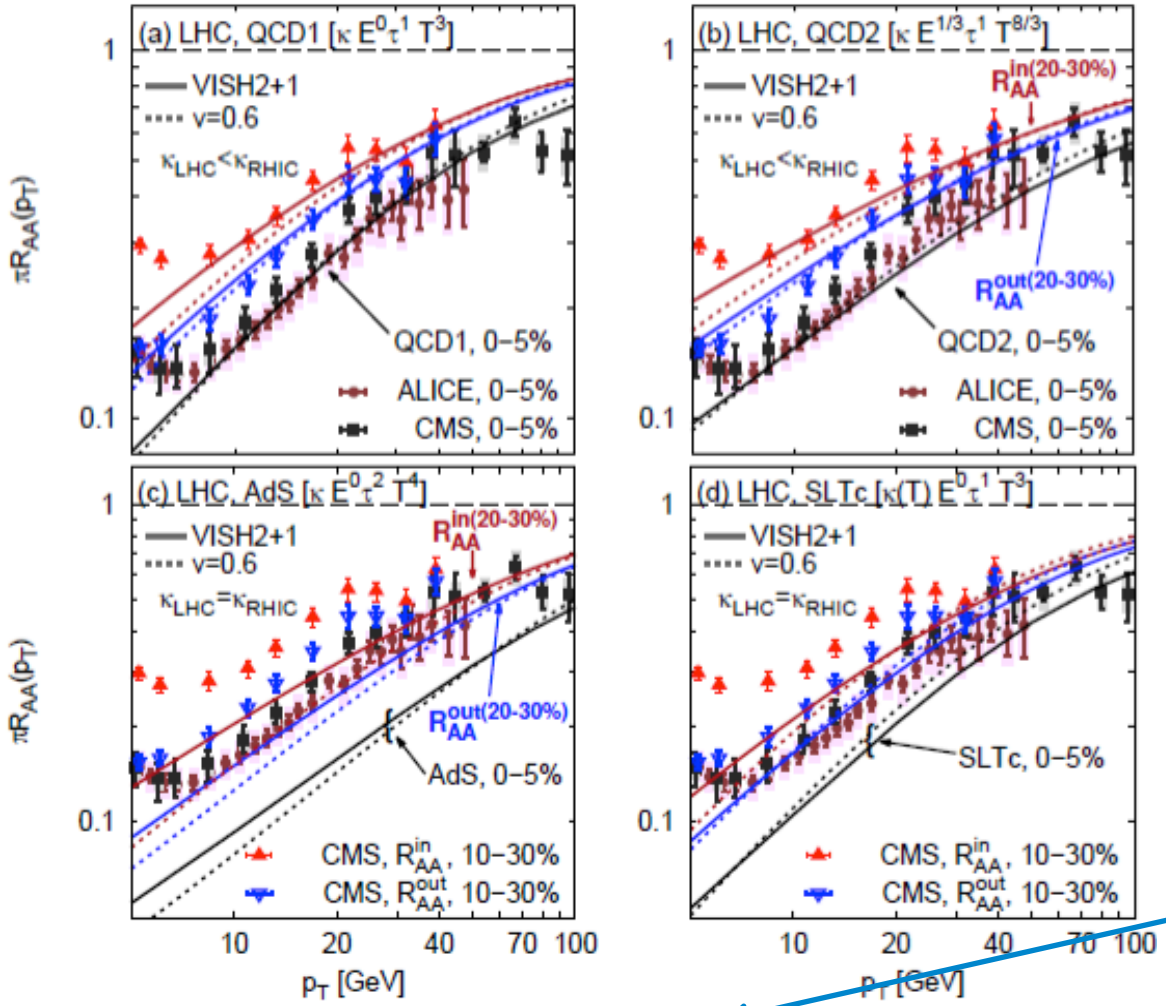

- (RHIC + LHC) & (RAA + v2) is a set of highly constraining observables for energy loss models
- After constrained parameters using pion RAA at RHIC and LHC, most jet energy loss models fail to reproduce the single particle high pT v2

$$dE/d\tau = -\kappa E^a \tau^b T^c$$

B. Betz, M. Gyulassy, arXiv: 1305.6458
New systematic studies of energy loss models using abc model wiith fluctuations added: B. Betz, M. Gyulassy, JHEP 1408, 090 (2014)

CUJET2.0: π^0 suppression w.r.t. reaction plane

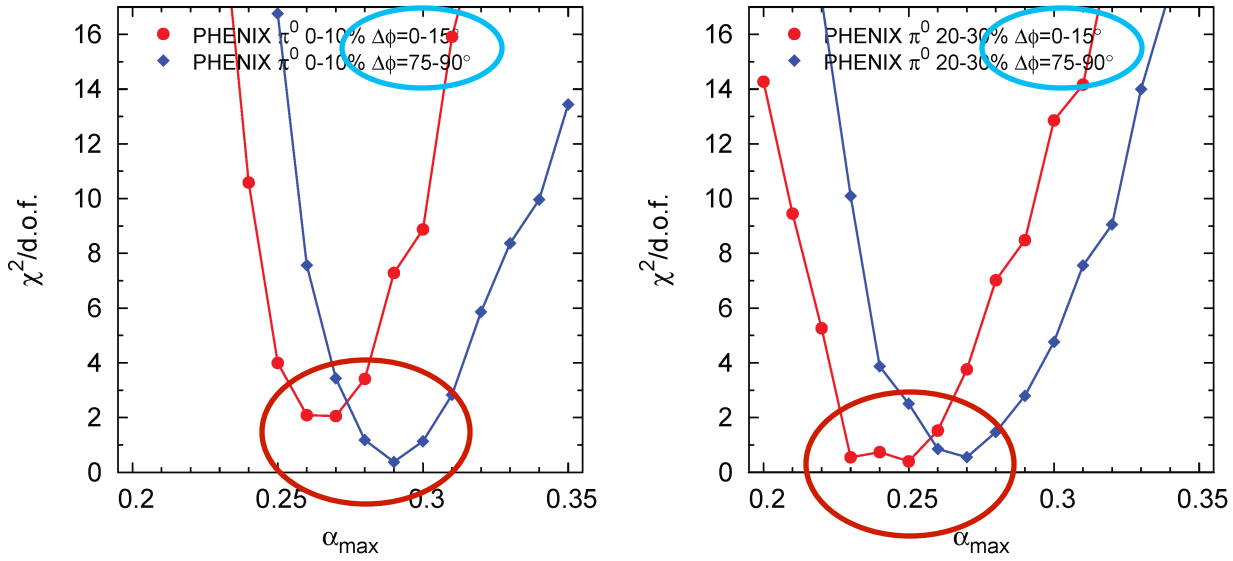

α_{max}	RHIC $\tilde{\chi}^2 < 1$	LHC $\tilde{\chi}^2 < 1$	RHIC $\tilde{\chi}^2 < 2$	LHC $\tilde{\chi}^2 < 2$
$b = 2.4$ fm	0.28-0.32	0.24-0.27	0.26-0.35	0.23-0.28
$b = 7.5$ fm	0.23-0.29	0.23-0.25	0.22-0.31	0.22-0.27

- Choose $\alpha_{max} = 0.23$ $(7.5fm + IN)$, 0.26 $(7.5fm + OUT)$, 0.26 $(7.5fm + IN)$, 0.29 $(7.5fm + OUT)$, the average R_{AA} falls within respective $\chi^2/d.o.f. <$ 2 window, while R_{AA}^{in} and R_{AA}^{out} are in perfect agreements with RHIC data
- As less as 10% azimuthal variation of path averaged α_{max} can account for the underestimated gap between R_{AA}^{in} and R_{AA}^{out} at RHIC
- Interesting ordering: in terms of naive path length from the origin, $7.5fm + IN < 7.5fm + OUT \approx 2.4fm + IN < 2.4fm + OUT$, the corresponding α_{max}: $0.23 < 0.26 = 0.26 < 0.29$.
- Model is fully constrained at RHIC, how about extrapolation to LHC?

CUJET2.0: high pT v2 with reaction plane dependent couplings

$$\begin{cases} R_{AA}^{in}(p_T) \approx R_{AA}^{h}(1+2v_2) \\ R_{AA}^{out}(p_T) \approx R_{AA}^{h}(1-2v_2) \end{cases},$$

$$v_2(p_T) = \frac{1}{2}\frac{R_{AA}^{in}(p_T) - R_{AA}^{out}(p_T)}{R_{AA}^{in}(p_T) + R_{AA}^{out}(p_T)}$$

- Extrapolation to LHC fits v2!
  - RAA is compatible with data in this anisotropic amax scenario as well
- As less as a 10% increase of the path averaged coupling strength from in- to out-of-reaction plane can simultaneously describe RAA and v2 at both RHIC and LHC
  - The azimuthal anisotropy is very sensitive to local temperature dependent jet-medium coupling

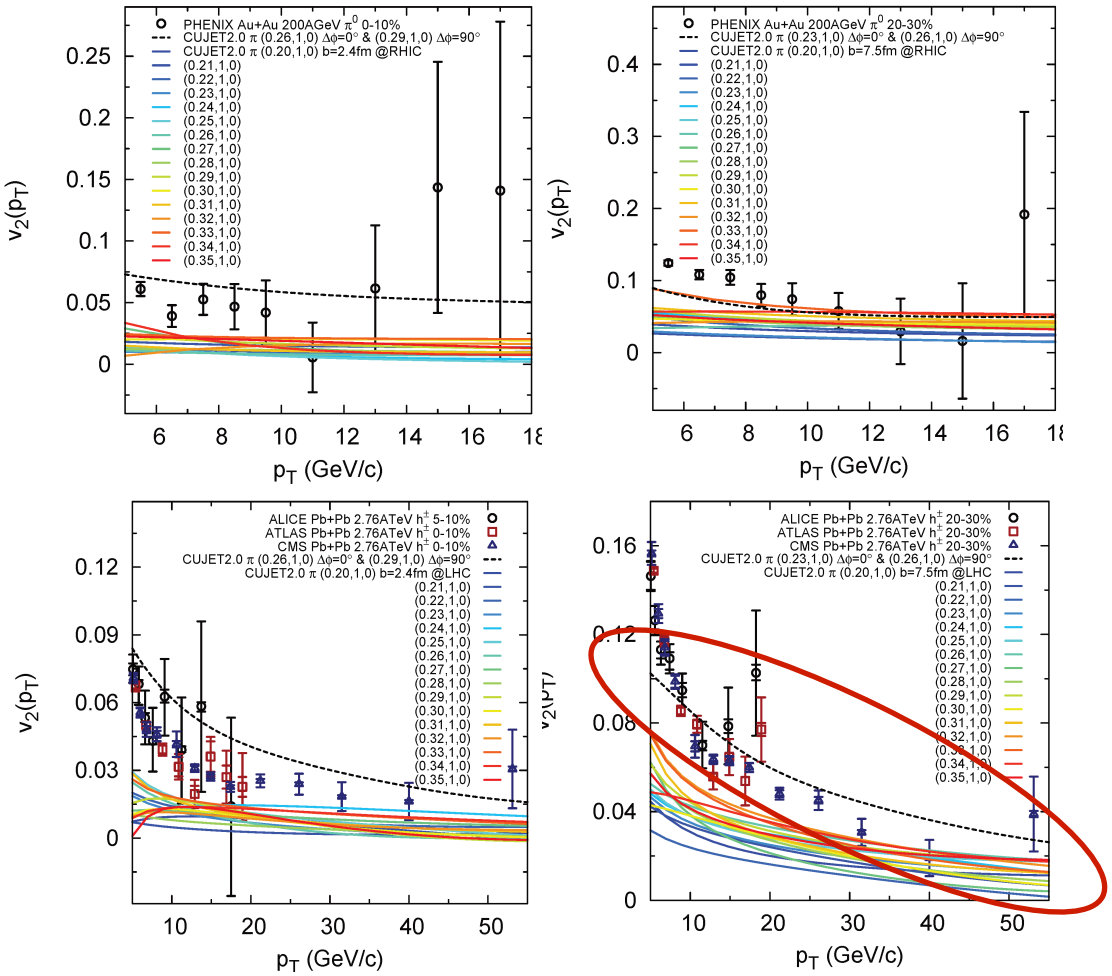

$\chi^2/d.o.f.$ ($b = 7.5$ fm)	v_2, RHIC	v_2, LHC	R_{AA}, RHIC	R_{AA}, LHC
$\alpha_{max}^{in} = 0.23$, $\alpha_{max}^{out} = 0.23$	3.72	43.03	0.93	0.73
$\alpha_{max}^{in} = 0.26$, $\alpha_{max}^{out} = 0.26$	2.06	24.89	0.23	1.06
$\alpha_{max}^{in} = 0.23$, $\alpha_{max}^{out} = 0.26$	0.50	4.92	0.42	0.54

JX, Buzzatti, Gyualssy, JHEP 1408, 063 (2014)

Coupling from Transparency to Opaqueness

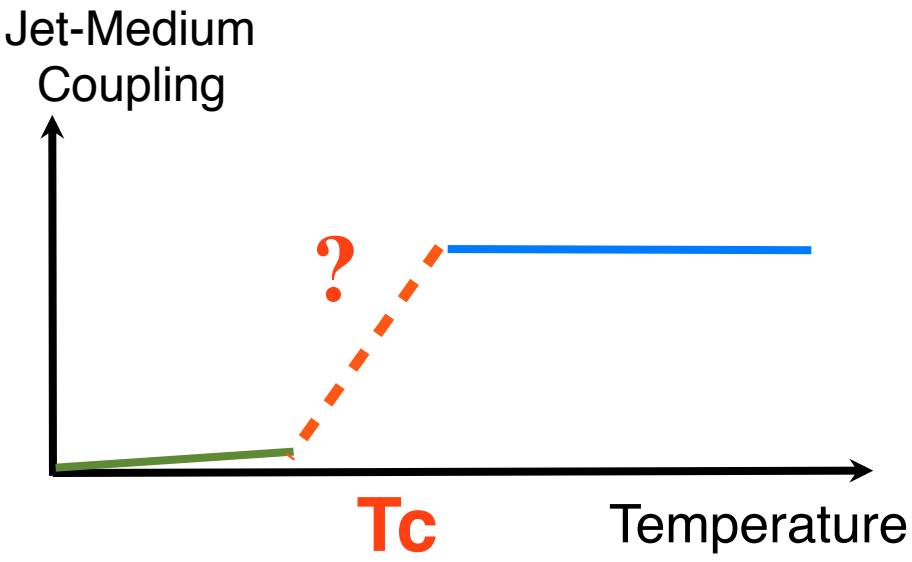

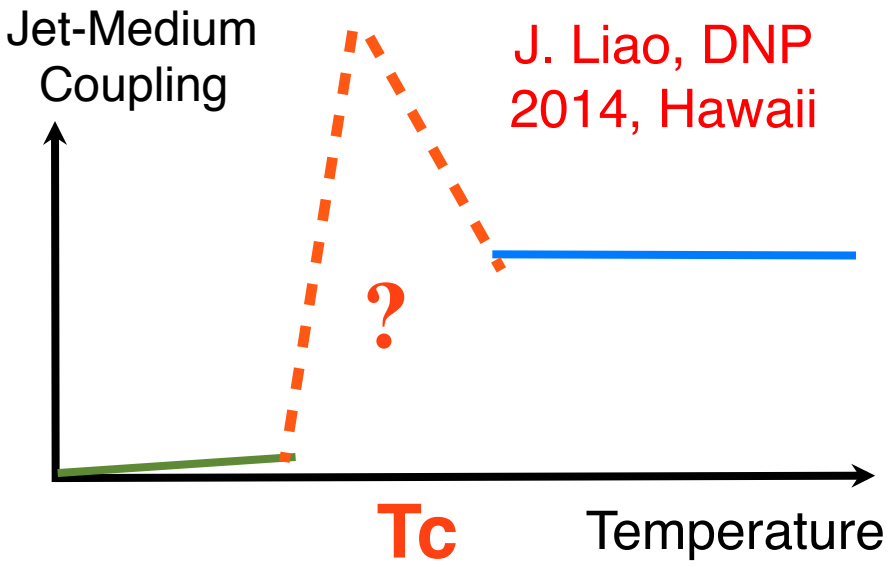

"Waterfall" scenario

"Volcano" scenario

- How does jet opacity for T>>Tc connect to jet transparency for T<<Tc?
- Can jet transparency for T<<Tc be reconciled with color confinement below Tc and perfect fluidity near Tc?

Dual Superconductivity

- Dual superconductivity is a promising mechanism for quark confinement. [Y.Nambu (1974). G.'t Hooft, (1975). S.Mandelstam, (1976) A.M. Polyakov (1975)]

superconductor

- Condensation of electric charges (Cooper pairs)
- Meissner effect: Abrikosov string (magnetic flux tube) connecting monopole and anti-monopole
- Linear potential between monopoles

dual superconductor

- Condensation of magnetic monopoles
- Dual Meissner effect: formation of a hadron string (chromo-electric flux tube) connecting quark and antiquark
- Linear potential between quarks

Akihiro, Shibata, Trento 2013

Liao-Shuryak "E-M See-Saw" Scenario

T<< Lambda_QCD | T ~ Lambda_QCD | T>> Lambda_QCD

Vacuum: confined — **Tc** — sQGP — ***wQGP: screening*** — T

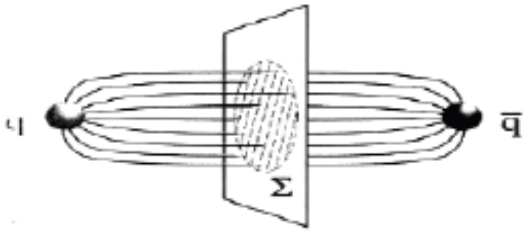

Electric Flux Tube:
Magnetic Condensate

Emergent plasma with E & M charges:
chromo-magnetic monopoles are the "missing DoF"

Plasma of E-charges
E-screening: g T
M-screening: g^2 T

$$L(\mathbf{x}) = \frac{1}{N_c}\mathrm{tr}\mathcal{P}\exp\left[ig\int_0^{1/T} A_4(\tau,\mathbf{x})d\tau\right]$$

$$\alpha_E * \alpha_M = 1.$$

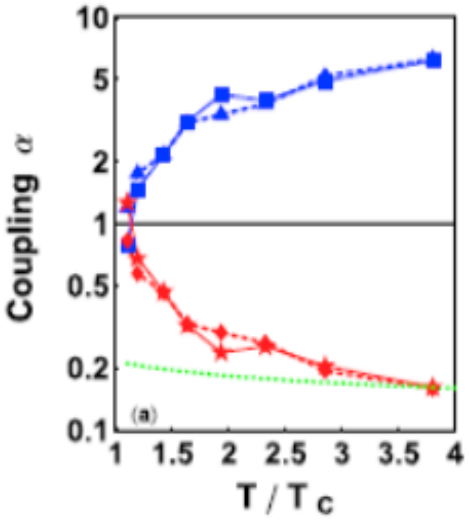

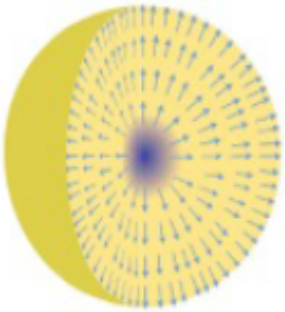

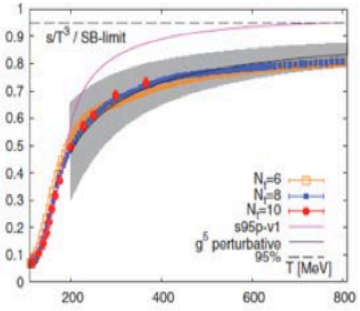

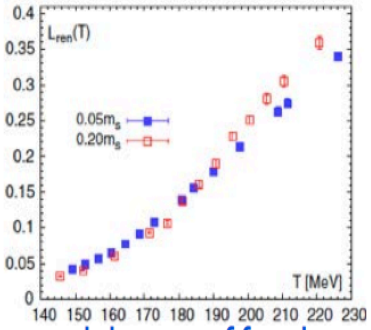

A region around Tc with liberated degrees of freedom
but only partially liberated color-electric objects—missing D.o.F:
semi-QGP + emergent magnetic component

JL & Shuryak:
Phys.Rev.C75:054907,2007; Phys.Rev.Lett.101:162302,2008;
Phys.Rev.C77:064905,2008; Phys.Rev.D82:094007,2010;
Phys.Rev.Lett.109:152001,2012.

Jet quenching in semi-Quark-Gluon-Monopole Plasmas

- CUJET3.0 = (Dynamical rc-DGLV + Elastic + (2+1)D Viscous Hydro)* + Magnetic Monopoles** + semi-Quark-Gluon Plasmas*** = CUJET2.0* + sQGMP

* JX, J. Liao and M. Gyulassy, arXiv:1411.3673 [hep-ph]
** J. Liao and E. Shuryak, PRL 102 (2009), PRL 101 (2008), PRC 75 (2007)
*** Y. Hidaka and R. D. Pisarski, PRD 78 (2008), 81 (2010)

- Solve the high pT v2 problem while retaining RAA consistency AND provides a quantitative new connection between a Tc enhanced jet transport qhat(E>10GeV, T) field and minimal viscosity eta/s ~ T^3/qhat(E→3T,T) → 0.1 near T → Tc

CUJET3.0 -- arXiv:1411.3673

Anisotropic Jet Quenching in semi-Quark-Gluon Plasmas with Magnetic Monopoles in Ultrarelativistic Heavy Ion Collisions

Jiechen Xu,[1] Jinfeng Liao,[2,3] and Miklos Gyulassy[1]
[1]*Department of Physics, Columbia University, 538 West 120th Street, New York, NY 10027, USA*
[2]*Physics Dept and CEEM, Indiana University, 2401 N Milo B. Sampson Lane, Bloomington, IN 47408, USA*
[3]*RIKEN BNL Research Center, Bldg. 510A, Brookhaven National Laboratory, Upton, NY 11973, USA*
(Dated: November 14, 2014)

CUJET3.0 = CUJET2.0 + semi-QGP + mag. monopoles

We now include both color-electric and color-magnetic scattering centers.

Original DGLV has only quark/gluon scattering centers

$$\frac{dE}{dx} \propto \ldots \int_{q^2} \left[\frac{n_e \left(\alpha_s(q^2)\alpha_s(q^2)\right) f_E^2}{q^2(q^2+f_E^2\mu^2)} + \frac{n_m \left(\alpha_s^e(q^2)\alpha^m(q^2)\right) f_M^2}{q^2(q^2+f_M^2\mu^2)} \right] \ldots$$

$$\frac{dE}{dx} \propto \ldots \int_{q^2} \frac{n_e\, \alpha_s^2(q^2)\, f_E^2}{q^2(q^2+f_E^2\mu^2)} \ldots$$

$$\frac{dE}{dx} \propto \ldots \int_{q^2} \frac{n_T}{(q^2+f_E^2\mu^2)(q^2+f_M^2\mu^2)} \times \kappa(q^2,T)$$

=1, by Dirac Quantization

$$\kappa(q^2,T) \equiv \alpha_s^2(q^2)\chi_T \left(f_E^2 + \frac{f_E^2 f_M^2 \mu^2}{q^2}\right) + (1-\chi_T)\left(f_M^2 + \frac{f_E^2 f_M^2 \mu^2}{q^2}\right)$$

$$\chi_T = c_q L + c_g L^2$$

Polyakov Loop suppressed color electric component

$$f_E = \sqrt{\chi_T}$$

$$f_M = C_m g_T$$

$$L(\mathbf{x}) = \frac{1}{N_c}\mathrm{tr}\mathcal{P}\exp\left[ig\int_0^{1/T} A_4(\tau,\mathbf{x})d\tau\right]$$

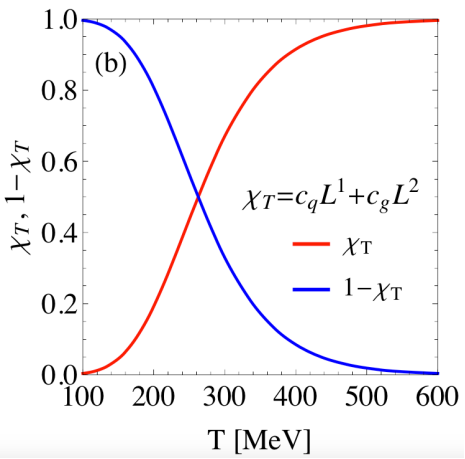

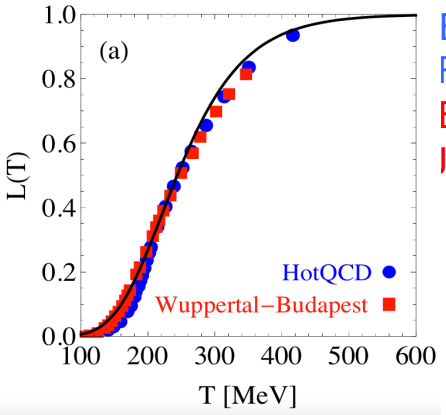

Bazavov et al., PRD 80 (2009)

Borsanyi et al., JHEP 09 (2010)

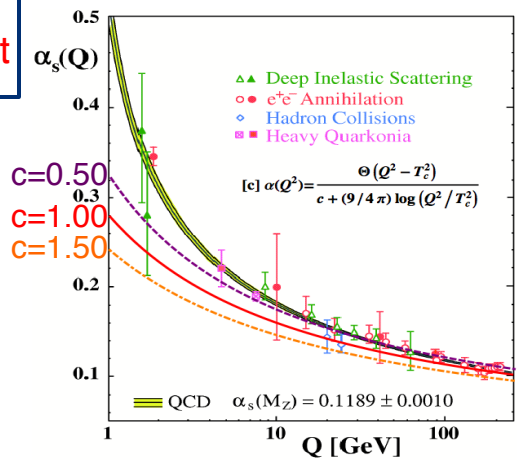

$$\alpha_s^2(q^2) \approx \left[1/\left[c + (9/2\pi)Log(q/\Lambda)\right]\right]^2$$

Polyakov Loop, EOS, Screening Masses

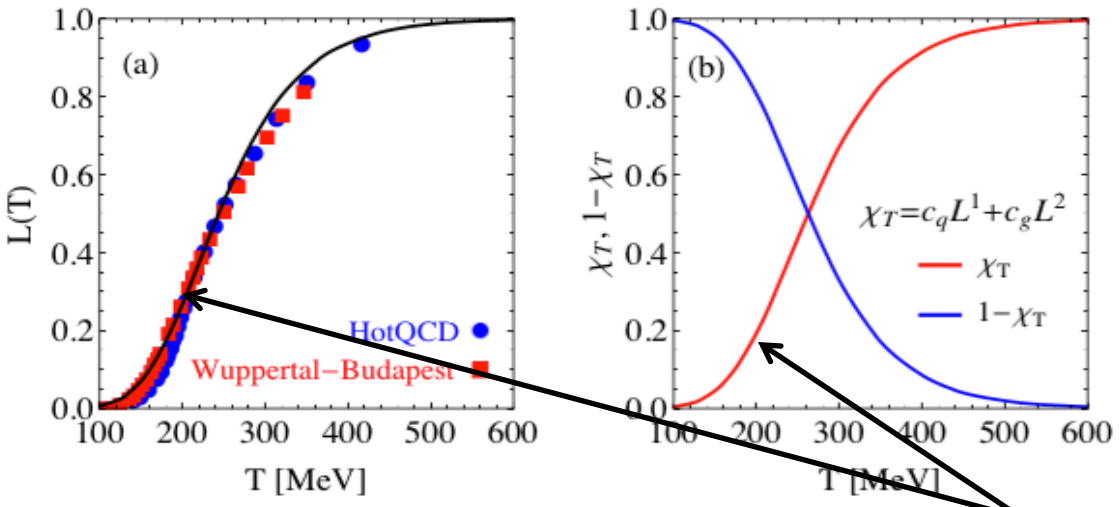

$$L(\mathbf{x}) = \frac{1}{N_c}\mathrm{tr}\mathcal{P}\exp\left[ig\int_0^{1/T} A_4(\tau,\mathbf{x})d\tau\right]$$

FIG. 1: (Color online) (a) The Polyakov loop $L(T)$ parameterization of Eq.(8) compared with lattice data from the HotQCD [54] and Wuppertal-Budapest Collaboration [55]; (b) The relative ratios of electric (red, $\chi(T)$) and magnetic (blue, $1-\chi(T)$) quasi-particles in the QCD matter. (c) The EOS from HotQCD (gray band: lattice data, dashed black: parametrization, both in [56]) as well as the number density of E (red) and M (blue) components at various temperatures. (d) The temperature dependence of the screening mass μ_E/T (red, electric) and μ_M/T (blue, electric) in CUJET3.0 compared with lattice calculation [57].

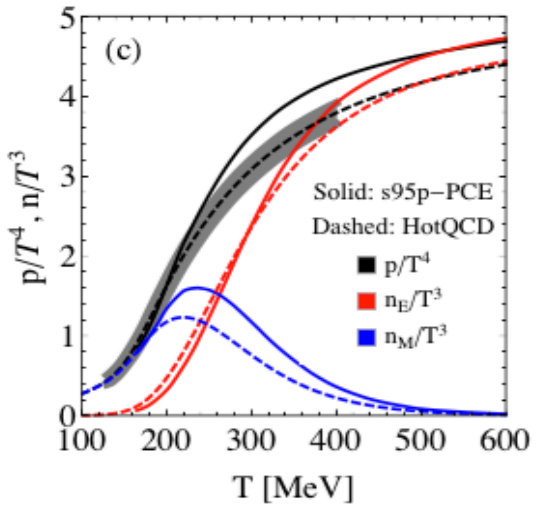

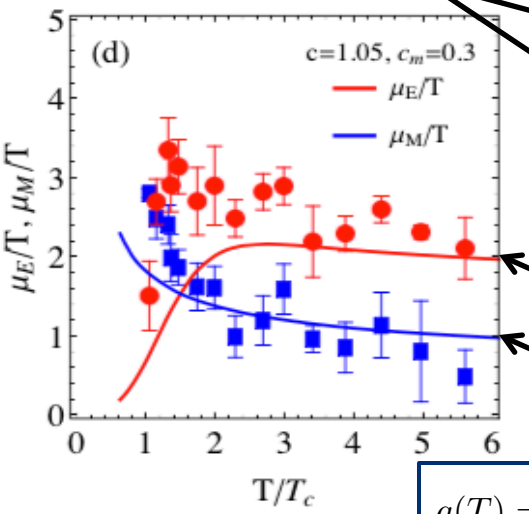

$$L(T) = \left[\tfrac{1}{2} + \tfrac{1}{2}Tanh[0.00769(T-72.6)]\right]^{10}$$

$$\chi_T = c_q\, L + c_g\, L^2$$

$$\mu_E^2 \sim \alpha_E n_E/T$$

$$f_E = \mu_E/\mu = \sqrt{\chi_T}$$
$$f_M = \mu_M/\mu = c_m g$$

$$g(T) = \sqrt{4\pi\alpha_s(\mu^2(T))} = \mu(T)/(T\sqrt{N_c/3 + N_f/6})$$

Peshier, hep-ph/0601119

JX, J. Liao, M. Gyulassy, arXiv:1411.3673

- The CUJET3.0 implementations of electric and magnetic components are well constrained by available lattice data.

CUJET3.0 accounts for (RHIC+LHC)*(R_{AA}+v_2)!

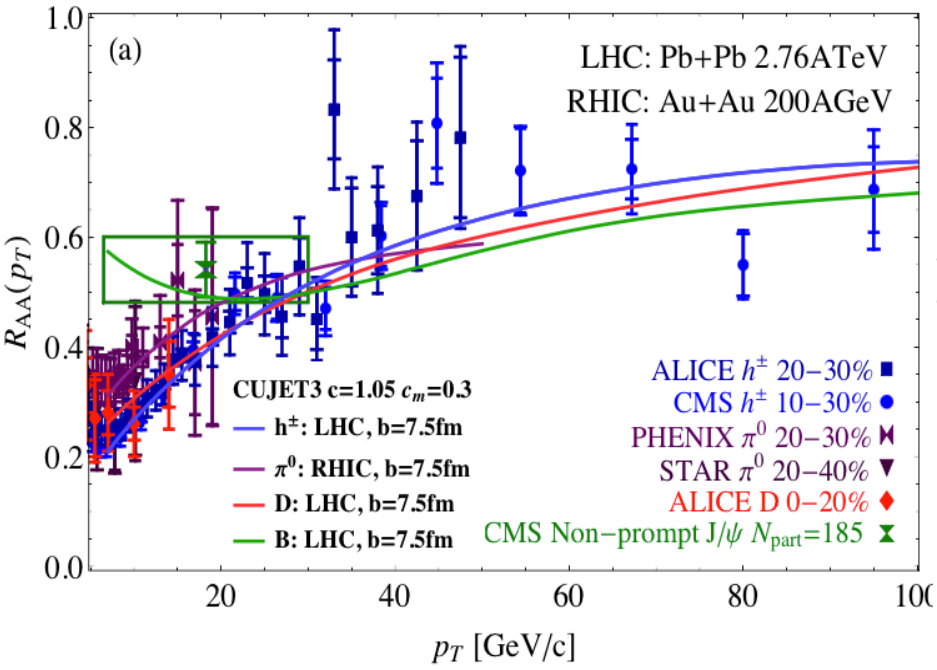

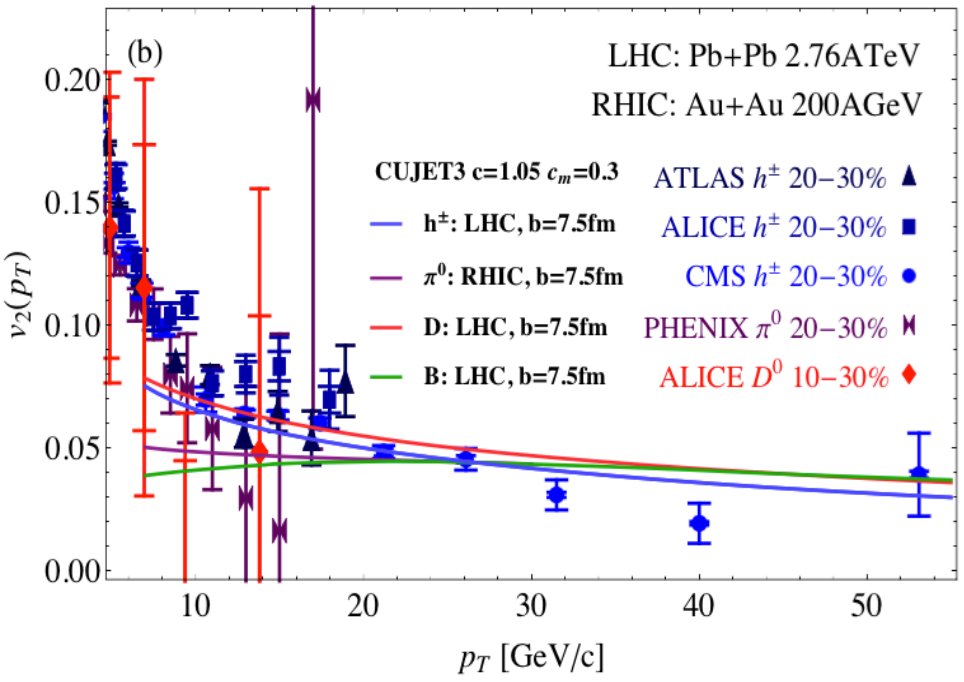

JX, J. Liao, M. Gyulassy, arXiv:1411.3673

The combined set of observables

(RHIC+LHC)*(R_{AA}+V_2)*(pion+D+B)

are consistently accounted for (within present experimental errors) in the CUJET3.0 framework using lattice QCD constrained near-Tc enhanced jet coupling to a VISH2+1 evolved semi-QGMP that approaches HTL sQGP at high T>3Tc

Open charm and beauty high p_T R_{AA} and v_2 at RHIC and LHC from CUJET3.0

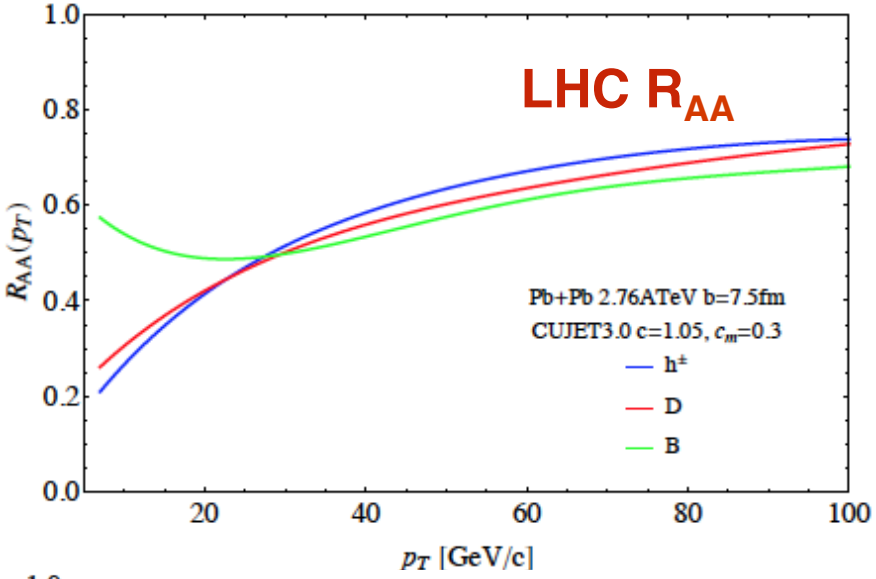

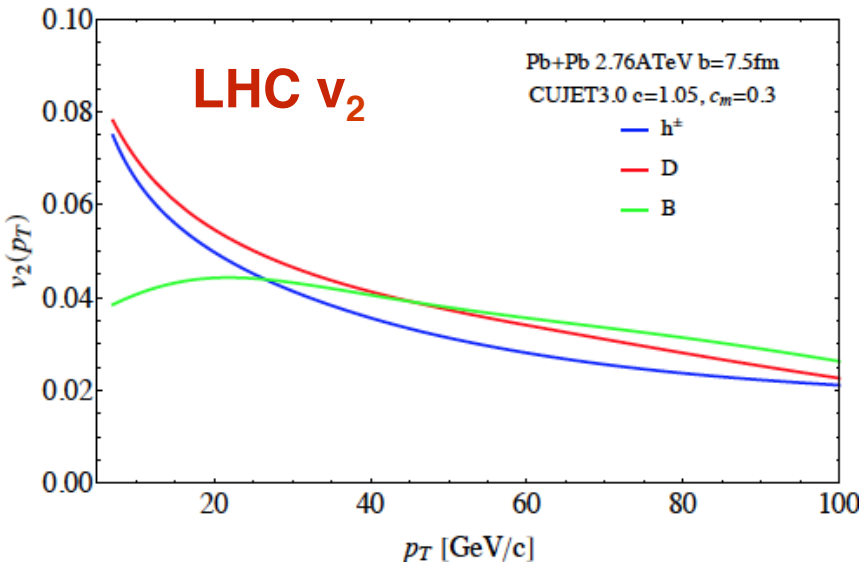

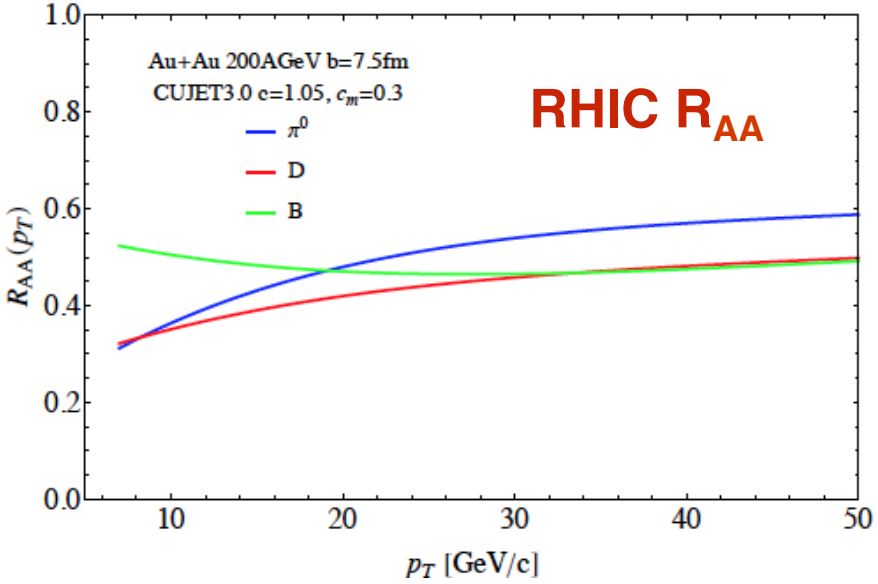

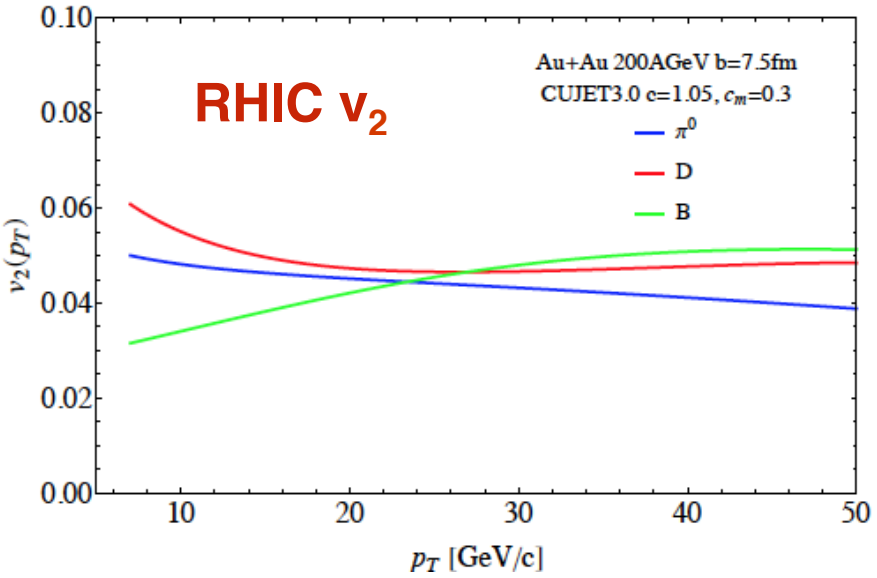

CUJET3.0: qhat(E,T) for quark jets in a sQGMP

Liu et al.PRL 2006 →

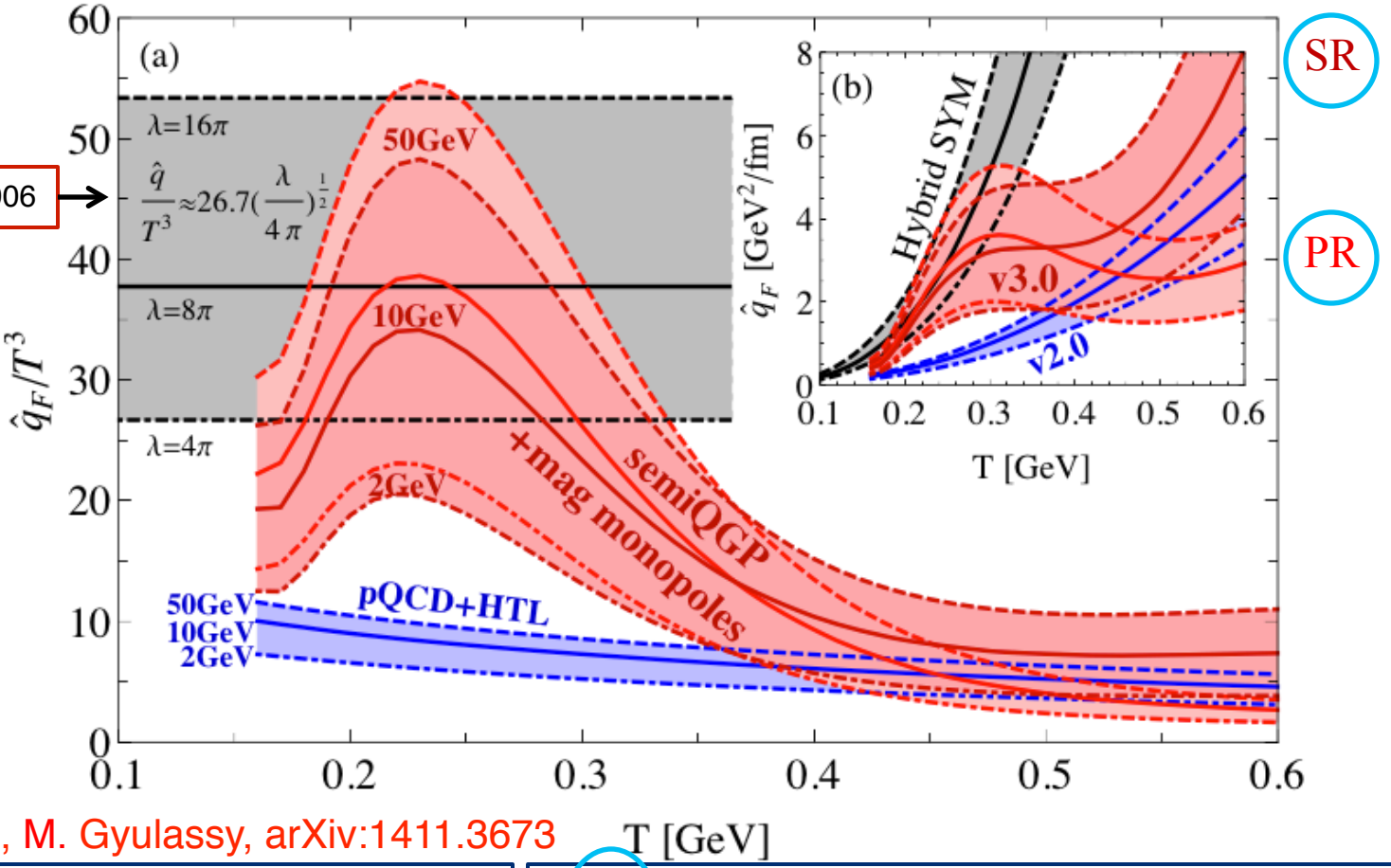

JX, J. Liao, M. Gyulassy, arXiv:1411.3673

$$\hat{q}_F = \int_0^{6ET} dq^2 \frac{2\pi q^2}{(q^2+f_E^2\mu^2)(q^2+f_M^2\mu^2)}\rho(T)$$
$$\times \left[(C_{qq}f_q + C_{qg}f_g)\alpha_s^2(q^2) + C_{qm}(1-f_q-f_g)\right]$$
$$\rho(T) \sim p(T)/T$$ p(T) from s95p-PCE EOS

$$\text{PR scheme}: f_q = c_q L(T),\ f_g = c_g L(T)^2,$$
$$\text{SR scheme}: f_q = c_q L(T)/N_s,\ f_g = c_g L(T)^2/N_s$$
$$N_s(T) = [s(T)/4]/[\pi^2 T^3(16+10.5N_f)/90]$$

- CUJET3.0 solution exhibits a “volcano” interpolation of qhat/T^3 between strong “AdS-like” sQGP at T=200-350MeV to more transparent “HTL-like” CUJET2.0 for T>400MeV

CUJET3.0: η/s vs T

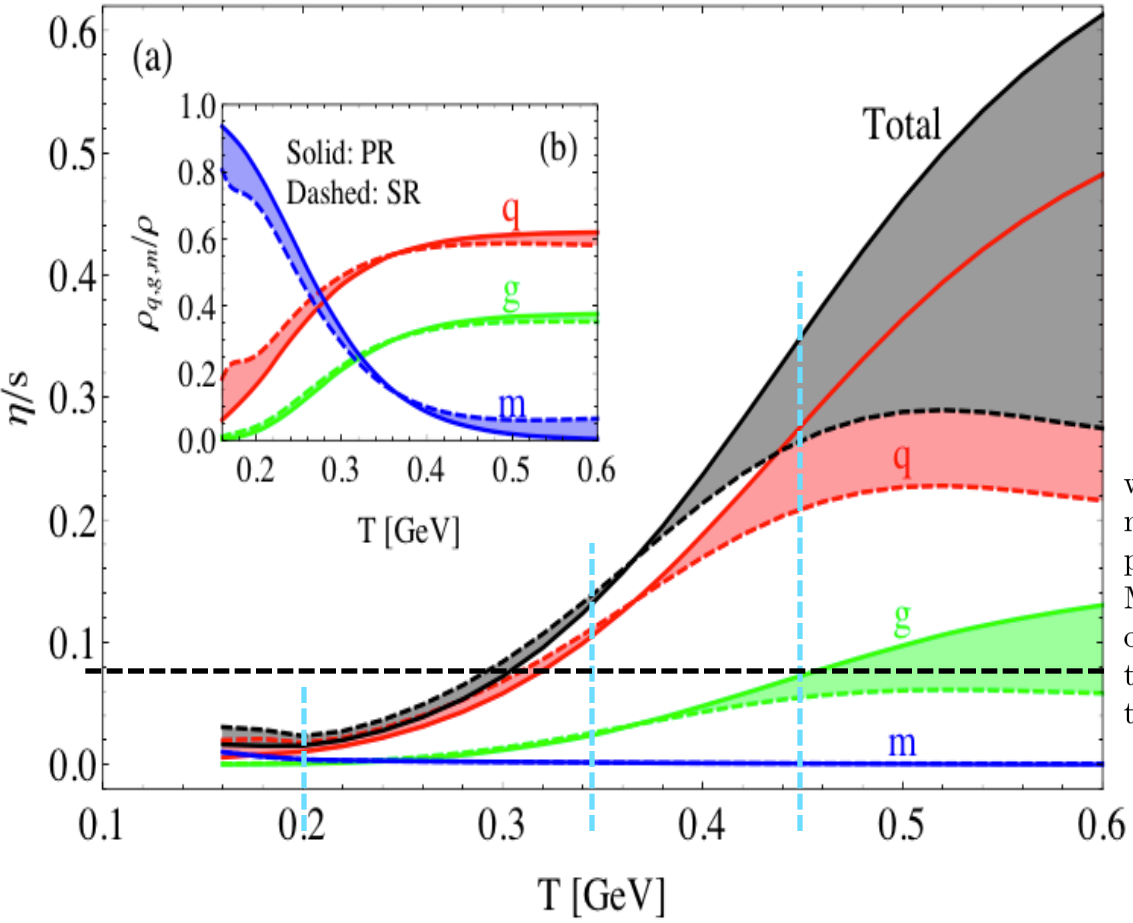

It is of special interest to utilize $\hat{q}_F(T,E)$ for an estimate of shear viscosity per entropy density η/s with kinetic theory formula as in [74–76]

$$\eta/s = \frac{1}{s}\frac{4}{15}\sum_a \rho_a \langle p\rangle_a \lambda_a^{tr}$$
$$= \frac{4T}{5s}\sum_a \rho_a \left(\sum_b \rho_b \int_0^{\langle \mathcal{S}_{ab}\rangle/2} dq^2 \frac{4q^2}{\langle \mathcal{S}_{ab}\rangle}\frac{d\sigma_{ab}}{dq^2}\right)^{-1}$$
$$= \frac{18T^3}{5s}\sum_a \rho_a/\hat{q}_a(T, E=3T) \quad , \qquad (15)$$

where we extrapolated $\hat{q}(T,E)$ down to the average thermal energy scale $E \sim 3T$ and denote by $\rho_a(T)$ the quasi-parton density of type $a = q, g, m$. The mean thermal Mandelstam variable $\langle \mathcal{S}_{ab}\rangle \sim 18T^2$. The contributions of $a = q, g, m$ to η/s are shown in Fig. 4(a), with the factions of quasi-parton densities shown in Fig. 4(b) using the schemes in Eq. (13). The $\hat{q}_{a=g,m}$ for adjoint gluons

JX, J. Liao, M. Gyulassy, arXiv:1411.3673

c.f. Danielewicz, Gyulassy, PRD 1985;
Hirano, Gyulassy, NPA 2006;
Majumder, Muller, Wang, PRL 2007

- Near η/s~1/4π in 160<T<300MeV dominated by jet+monopole scatterings
- Grows to η/s~0.16-0.18@350MeV, η/s~0.24-0.32@450MeV,
- Below Tc magnetic monopoles condensate and sQGMP becomes high η/s hadron resonance gas (but HRG not yet been implemented in CUJET3.0)

Near-Tc Properties of sQGMP are Special!

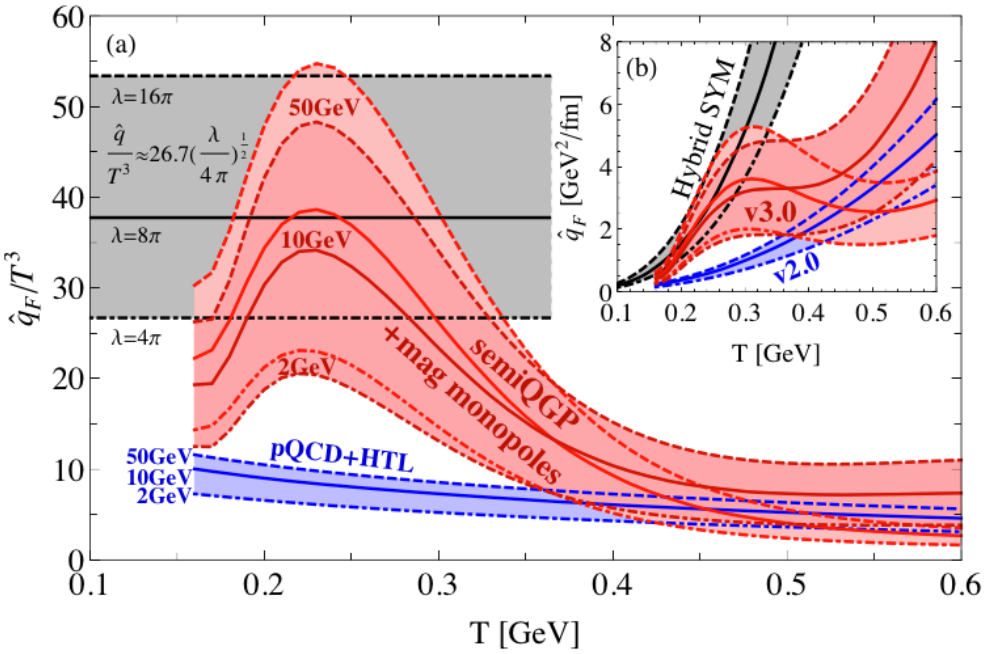

Jet transport coefficient qhat/T³ computed from CUJET3.0 shows a prominent peak near Tc!

Shear viscosity, η/s, computed from CUJET3.0 shows a clear minimum near Tc and rapid rise at high T!

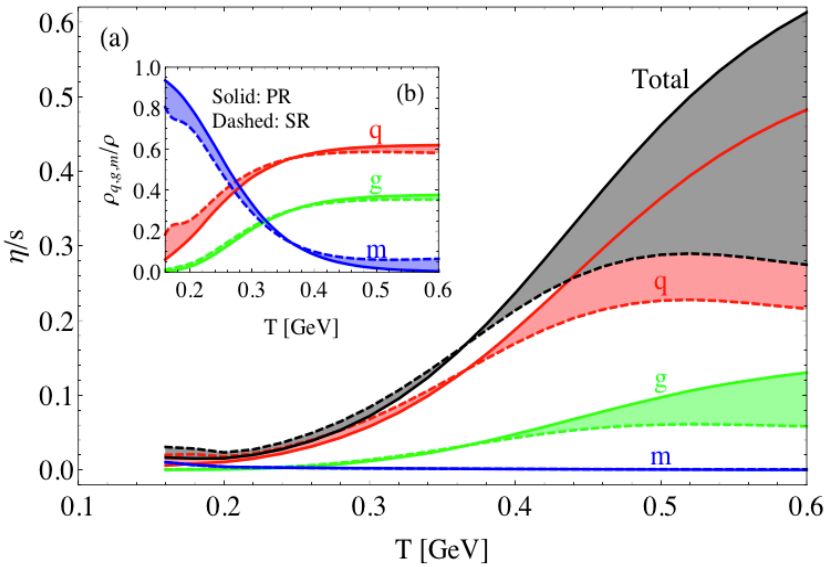

BES@RHIC and LHC are both essential to constrain and map out the strongly non-conformal QCD confinement transition physics, allowing full exploration of the parton-hadron transition matter that is the most perfect and the most color-opaque liquid!

JX, J. Liao, M. Gyulassy, arXiv:1411.3673

Summary

- CUJET is a solution to both the “heavy quark puzzle” and the “surprising transparency of QGP at LHC”

- $R_{AA}(p_T)$ of B meson is predicted to have a robust intersection with π^0 or $h^{\pm}$ in the p_T range of 30-40GeV/c from CUJET

- Introducing running coupling accounts for RHIC and LHC R_{AA} simultaneously, but leads to a 50% underestimate of v_2. A 10% increase in the path averaged coupling from in- to out-of-reaction plane paths can remove this discrepancy.

- With pQCD + semi-QGP + magnetic monopoles, CUJET3.0 describes (RHIC+LHC) × (R_{AA}+v_2) × (pion+D+B) simultaneously
  - qhat from CUJET3.0 smoothly bridges the AdS holography limit near Tc and the HTL pQCD limit at high T
  - eta/s from CUJET3.0 approaches the perfect fluidity ~0.1 near Tc, and rises rapidly at high T

Thank you for your attention!

Backup

Convergence of the DGLV opacity series

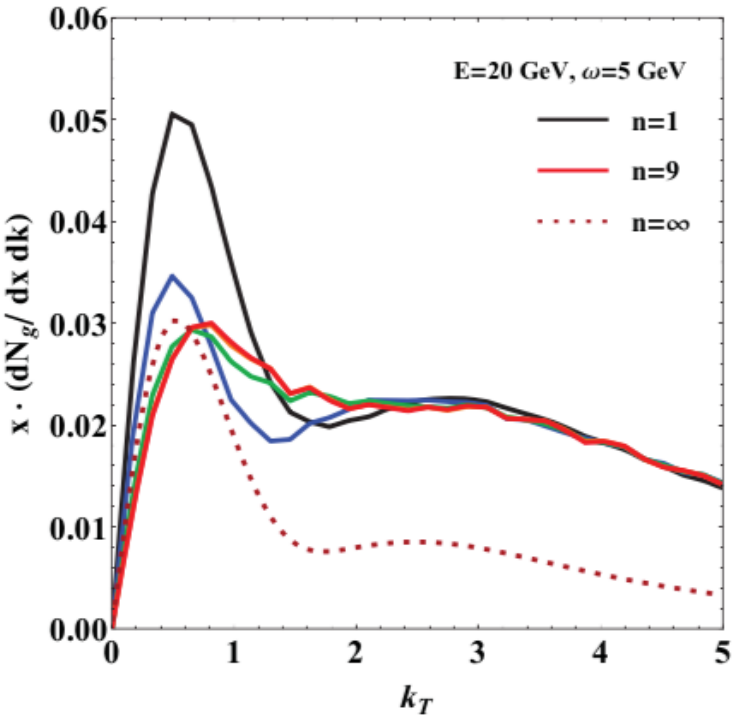

Figure 15. Radiated gluon transverse momentum distribution for a heavy quark jet with energy $E = 20\,\mathrm{GeV}$ traversing a brick plasma of size $L = 5\,\mathrm{fm}$ emitting a gluon with energy $\omega = 5\,\mathrm{GeV}$. The mass of the quark $M = 4.75\,\mathrm{GeV}$. The DGLV opacity series calculated up to n=1 (black), 3 (blue), 5 (green), 7 (orange), 9 (red) are shown in the figure. The opacity expansion computed up to ninth order is shown to converge to the ASW multiple soft scattering limit (maroon, dashed) for small $k_\perp \lesssim \hat{q}L \approx 1\,\mathrm{GeV}$. At large $k_\perp$, differs from the ASW limit, DGLV has a robust Laudau tail. Other parameters used in the simulation are: $\lambda = 1.16\,\mathrm{fm}$, $\mu = 0.5\,\mathrm{GeV}$, $m_g = 0.356\,\mathrm{GeV}$, $T = 0.258\,\mathrm{GeV}$, $n_f = 0$, $\alpha_s = 0.3$.

JX, Buzzatti, Gyulassy, JHEP 1408, 063 (2014)

Heavy Quark Puzzle: The Dead Cone

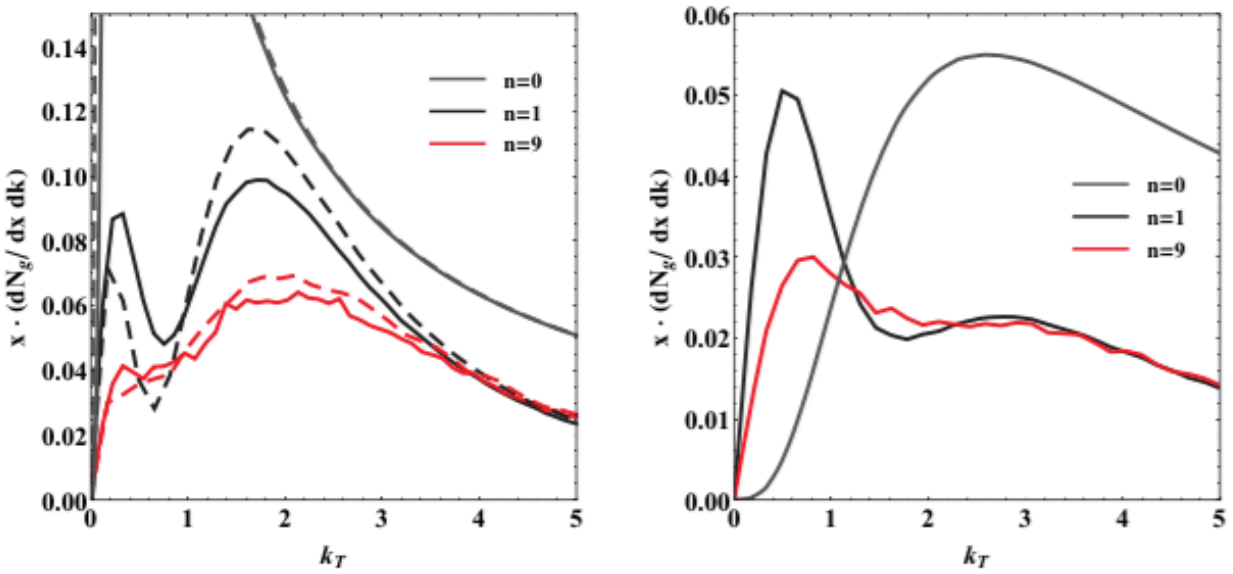

Figure 18. Radiation spectrum for charm (*left*) and bottom (*right*) quarks traversing a brick of thickness $L = 5\,\mathrm{fm}$, with $E = 20\,\mathrm{GeV}$ and $\omega = 5\,\mathrm{GeV}$ ($x = 0.25$). The masses are assumed $M_c = 1.2\,\mathrm{GeV}$ and $M_b = 4.75\,\mathrm{GeV}$. The dashed curves represent the spectrum of a light jet of mass $M_l = 0.2\,\mathrm{GeV}$. Notice the similarity between the light and charm spectra, as opposed to the bottom one. The vacuum spectrum radiation is added to the plot (gray curve), showing the radiation dead cone for respective quark jets. Other parameters used in the calculation are: $\lambda = 1.16\,\mathrm{fm}$, $\mu = 0.5\,\mathrm{GeV}$, $m_g = 0.356\,\mathrm{GeV}$, $T = 0.258\,\mathrm{GeV}$, $n_f = 0$, $\alpha_s = 0.3$.

$$x\frac{dN_g^0}{dxd\mathbf{k}} \sim \frac{\mathbf{k}^2}{(\mathbf{k}^2+\chi^2)^2}$$

$$\theta < \chi/\omega = \sqrt{M^2x^2 + m_g^2(1-x)}/(xE)$$

JX, Buzzatti, Gyulassy, JHEP 1408, 063 (2014)

Radiative vs Elastic

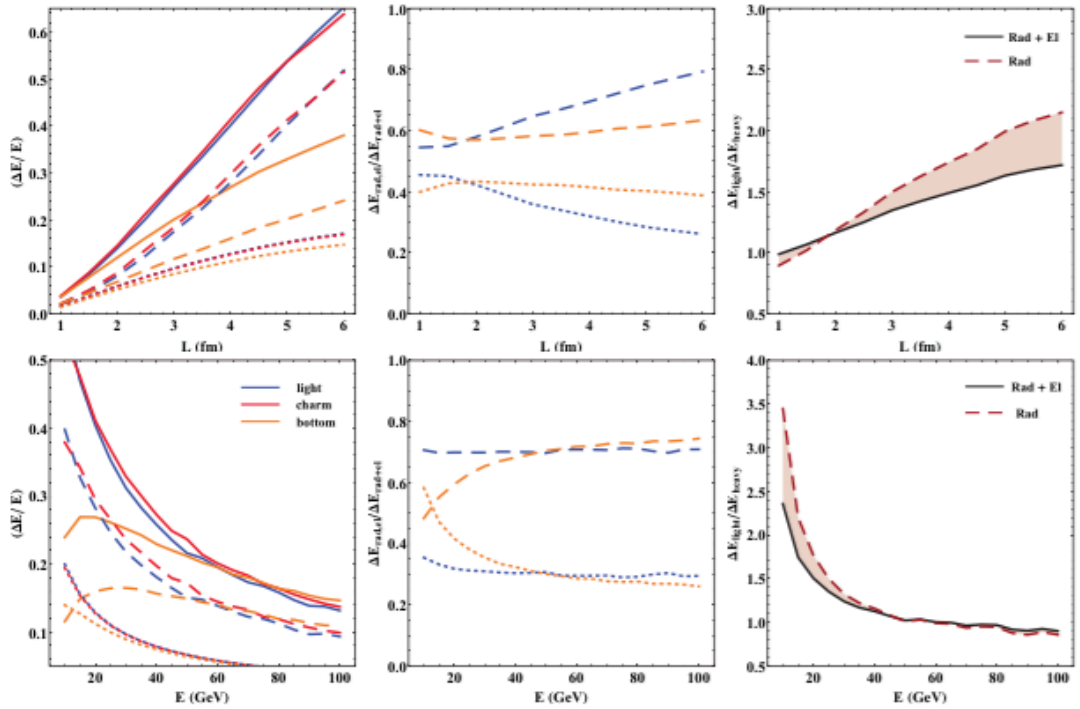

Figure 22. (LEFT panels) Radiative (dashed), elastic (dotted) and total (solid) energy loss for light (blue, $M = 0.2\,\mathrm{GeV}$), charm (red, $M = 1.2\,\mathrm{GeV}$) and bottom (orange, $M = 4.75\,\mathrm{GeV}$) quarks in a dynamical brick plasma of size L. The plasma is thermalized at temperature $T = 0.258\,\mathrm{GeV}$ and characterized by only gluonic degrees of freedom ($n_f = 0$). Poisson fluctuations for the radiative sector and Gaussian fluctuations for the elastic sector are taken into account. The total energy loss is calculated from the convolution of both sectors. TOP: the quark jet energy is set to $E = 20\,\mathrm{GeV}$. BOTTOM: $L = 4\,\mathrm{fm}$. (MIDDLE panels) Ratio $\Delta E_{\mathrm{rad}}/\Delta E_{rad+el}$ (dashed lines) and $\Delta E_{\mathrm{el}}/\Delta E_{rad+el}$ (dotted lines), for light (blue) and bottom (orange) quarks. ΔE_{rad+el} denotes the total energy loss. The ratios are computed from the results in the left panels. The dominant contribution to the total energy loss comes from inelastic collisions. (RIGHT panels) Light to bottom quark energy loss ratio, for radiative only (dashed) and total (solid) energy loss. The curves are obtained from the same data plotted in the left panels. Other parameters used in the calculations are: $\lambda = 1.16\,\mathrm{fm}$, $\mu = 0.5\,\mathrm{GeV}$, $m_g = 0.356\,\mathrm{GeV}$, $\alpha_s = 0.3$.

JX, Buzzatti, Gyulassy, JHEP 1408, 063 (2014)

Heavy quark puzzle: Where are the problems?

- Jet path length
- pp spectra
- Scattering centers recoil

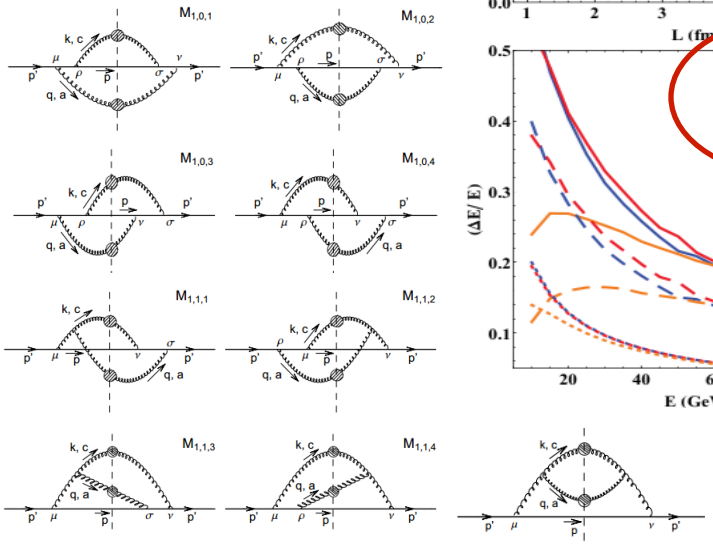

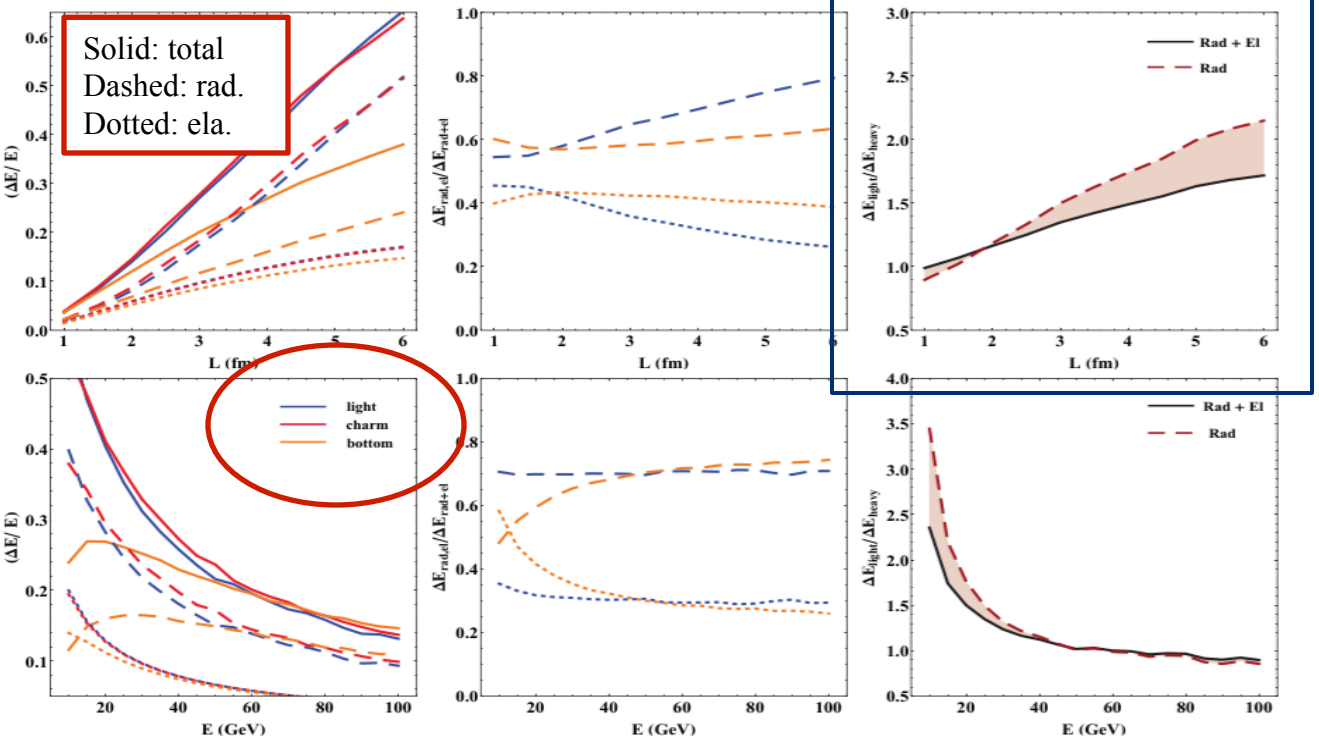

$$\lambda_{\rm dyn} \Longleftrightarrow \lambda_{\rm stat} = \frac{\lambda_{\rm dyn}}{c(n_f)}$$

$$\left[\frac{\mu^2}{q^2(q^2+\mu^2)}\right]_{\rm dyn} \Longleftrightarrow \left[\frac{\mu^2}{(q^2+\mu^2)^2}\right]_{\rm stat}$$

Djordjevic and Heinz, PRC (2008)

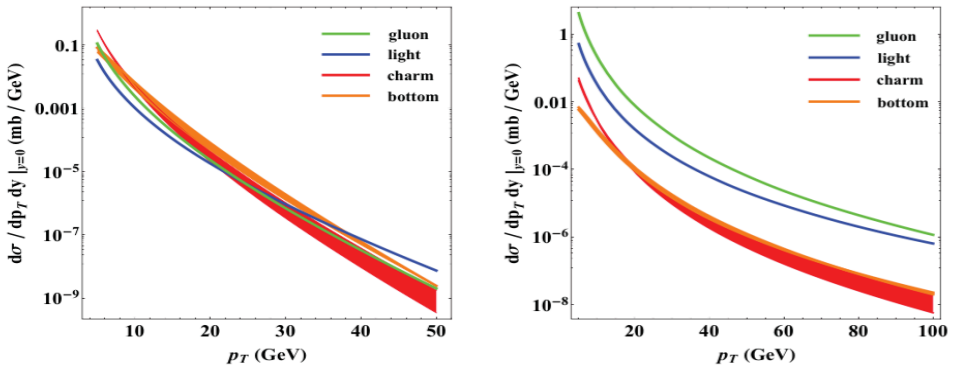

Figure 24. pQCD p+p production spectra at $\sqrt{s_{NN}} = 200\,\text{GeV}$ (RHIC, *left*) and $\sqrt{s_{NN}} = 2.76\,\text{TeV}$ (LHC, *right*). Notice how steeper the RHIC spectra are compared to LHC ones. The light

Pre-thermal Schemes

- Solid: Linear
- Dashed: Free Streaming
- Dotted: Divergent

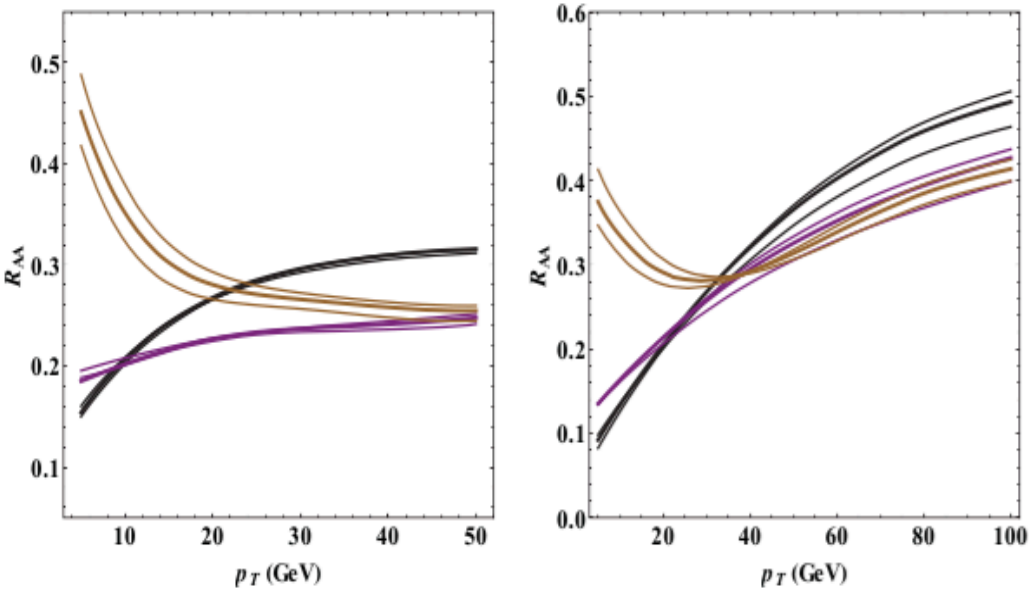

Figure 32. Flavor R_{AA} at RHIC (*left*) and LHC (*right*). In black the pions, in purple the D mesons, in brown the B mesons. Thick lines correspond to the linear thermalization model with $\alpha_s = 0.3$, thin lines represent both the divergent and free streaming models with $\alpha_s = 0.27, 0.32$ respectively. Results are calculated within the framework of fixed coupling CUJET1.0.

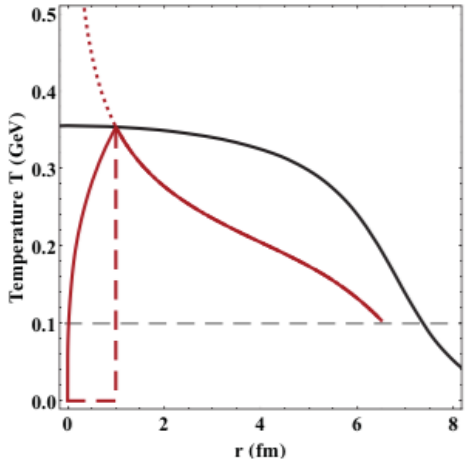

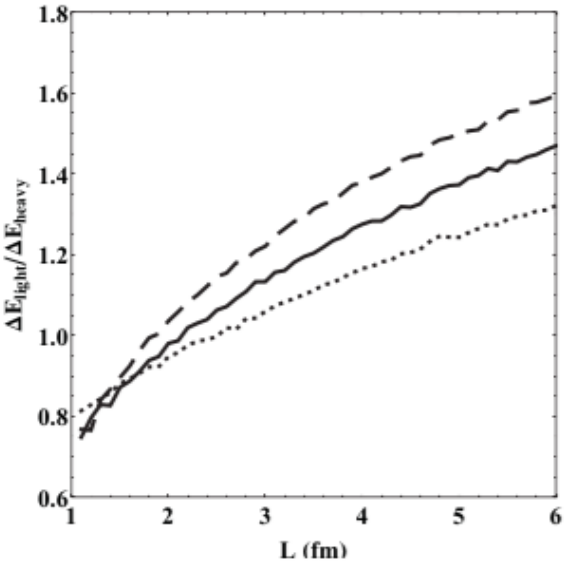

JX, Buzzatti, Gyulassy, JHEP 1408, 063 (2014)

Pre-CUJET1.0 = Dynamical fcDGLV + Elastic + Glauber

Radiative: dynamical DGLV

$$x_E \frac{dN_g^{n=1}}{dx_E}(\mathbf{x}_0,\phi) = \frac{18 C_R \alpha_s}{\pi^2}\frac{4+n_f}{16+9n_f}\int d\tau\, \rho(\mathbf{z}) \int d^2\mathbf{k} \int d^2\mathbf{q}\, \alpha_s^2 |\tilde{v}(\mathbf{q},\mathbf{z})|^2$$
$$\times \frac{-2(\mathbf{k}-\mathbf{q})}{(\mathbf{k}-\mathbf{q})^2+\chi^2(\mathbf{z})}\left(\frac{\mathbf{k}}{\mathbf{k}^2+\chi^2(\mathbf{z})} - \frac{(\mathbf{k}-\mathbf{q})}{(\mathbf{k}-\mathbf{q})^2+\chi^2(\mathbf{z})}\right)$$
$$\times \left(1-\cos\left(\frac{(\mathbf{k}-\mathbf{q})^2+\chi^2(\mathbf{z})}{2x_+E}\tau\right)\right)$$
$$\times \left(\frac{x_E}{x_+}\right) J(x_+(x_E))$$

$$|\tilde{v}(\mathbf{q},\mathbf{z})|^2 = \frac{f_E^2 - f_M^2}{(\mathbf{q}^2+f_E^2\mu^2(\mathbf{z}))(\mathbf{q}^2+f_M^2\mu^2(\mathbf{z}))}$$

$$\chi^2(\mathbf{z}) = M^2 x_+^2 + m_g^2(\mathbf{z})(1-x_+),\ m_g(\mathbf{z}) = \mu(\mathbf{z})/\sqrt{2}$$

$$\mu^2(\mathbf{z}) = g^2 f_E^2 T(\mathbf{z})^2\,(1+n_f/6) = 4\pi\alpha_s f_E^2 T(\mathbf{z})^2\,(1+n_f/6)$$

$$0 \le k_\perp \le x_E E\ ,\ 0 \le q_\perp \le \mathrm{Min}\{k_\perp, \sqrt{4ET(\mathbf{z})}\}$$

$$x_+(x_E) = \frac{1}{2}x_E\left(1+\sqrt{1-\left(\frac{k_\perp}{x_E E}\right)^2}\right) \qquad J(x_+(x_E)) \equiv \frac{dx_+}{dx_E} = \frac{1}{2}\left(1+\left(1-\left(\frac{k_\perp}{x_E E}\right)^2\right)^{-1}\right)$$

Elastic: Thoma-Gyulassy (TG)

$$\frac{dE(\mathbf{z})}{d\tau} = -C_R \pi \alpha_s^2 T(\mathbf{z})^2 \left(1+\frac{n_f}{6}\right)\log\left(\frac{4T(\mathbf{z})\sqrt{E(\mathbf{z})^2-M^2}}{\left(E(\mathbf{z})-\sqrt{E(\mathbf{z})^2-M^2}+4T(\mathbf{z})\right)\mu(\mathbf{z})}\right)$$

Improvements in CUJET1.0

Path length fluctuations

$$L(\vec{x}_\perp,\phi) = \int d\tau \rho_p(\vec{x}_\perp + \tau\hat{n}(\phi))/\langle\rho_p\rangle$$

$$P(\quad E_i \quad \to E_i - \Delta_{rad} - \Delta_{el}) = \int \frac{d\phi}{2\pi}\int \frac{d^2\vec{x}_\perp}{N_{bin}(b)} T_{AA}(\vec{x}_\perp,\vec{b}) \otimes P_{rad}\ (\Delta_{rad}; L(\vec{x}_\perp,\phi)) \otimes P_{el}(\Delta_{el}; L(\vec{x}_\perp,\phi)).$$

$$T(\mathbf{z})|_{\tau^{MAX}} = T_f$$

Power law assumption of heavy quark pQCD spectra

$$Ed^3\sigma_Q/d^3k \propto 1/p_T^{n+2}$$

$$R_Q^I = \int \frac{d\phi}{2\pi}\int \frac{d^2\vec{x}_\perp}{N_{bin}(b)} T_{AA}(\vec{x}_\perp,\vec{b}) \int d\epsilon(1-\epsilon)^n P_Q^I(\epsilon; L(\vec{x}_\perp,\phi)),$$

Assume Poisson distribution for the number of incoherently emitted gluons

Radiative energy loss fluctuations

$$P_{rad}(\epsilon) = P_0\delta(\epsilon) + \tilde{P}(\epsilon) + P_1\delta(\epsilon_{MAX} - \epsilon)$$

Elastic energy loss fluctuations

$$P_{el}(\epsilon) = e^{-\overline{N}_c}\delta(\epsilon) + \mathcal{N}e^{-\frac{(\epsilon-\overline{\epsilon})^2}{4T\overline{\epsilon}/E}}$$

Gaussian fluctuation for multiple collisions

Fragmentation

$$\frac{d\sigma^h}{dp}(p) = \sum_i \int_{p/p_{max}}^1 dx\ \frac{d\sigma^i}{dp}\left(\frac{p}{x}\right)\ D^{i\to h}\left(x;\frac{p}{x}\right)$$

Pressure/Entropy Counting & eta/s

- Extra factors come from quantum statistics which differ slightly from Stefan-Boltzmann
- Different counting schemes bring theoretical uncertainties

$$\rho(\mathbf{x}) = \sum \frac{\zeta(3)}{\pi^2} g_i \eta_i T^3(\mathbf{x})$$
$$\epsilon(\mathbf{x}) = \sum \frac{\pi^2}{30} g_i \eta_i' T^4(\mathbf{x})$$
$$p(\mathbf{x}) = \epsilon(\mathbf{x})/3$$
$$s(\mathbf{x}) = \frac{p(\mathbf{x}) + \epsilon(\mathbf{x})}{T} \approx \kappa \rho(\mathbf{x})$$

$$\frac{\eta}{s} = \frac{18}{5} \frac{T^3}{s(T)} \sum_a \frac{d_a(T)}{\sum_b d_b(T) F_{ab}(T)}$$

$$a, b = q, g, m$$

$$d_q = c_q \cdot L(T)\ (PR)\ or\ c_q \cdot L(T)/N_s\ (SR)$$

$$d_g = c_g \cdot L^2(T)\ (PR)\ or\ c_g \cdot L^2(T)/N_s\ (SR)$$

$$d_m = 1 - d_q - d_g$$

$$F_{ab}(T) = \int_0^{9T^2} dq^2 \frac{2\pi q^2 C_{ab} \alpha_a \alpha_b}{(q^2 + f_E^2 \mu^2)(q^2 + f_M^2 \mu^2)}$$

$$\alpha_q = \alpha_g = \alpha_E\ ,\ \alpha_m = 1/\alpha_E$$

$$C_{qq} = 4/9$$

$$C_{qg} = C_{gq} = C_{qm} = C_{mq} = 1$$

$$C_{gg} = C_{mm} = 9/4$$

More about the multi-scale running coupling

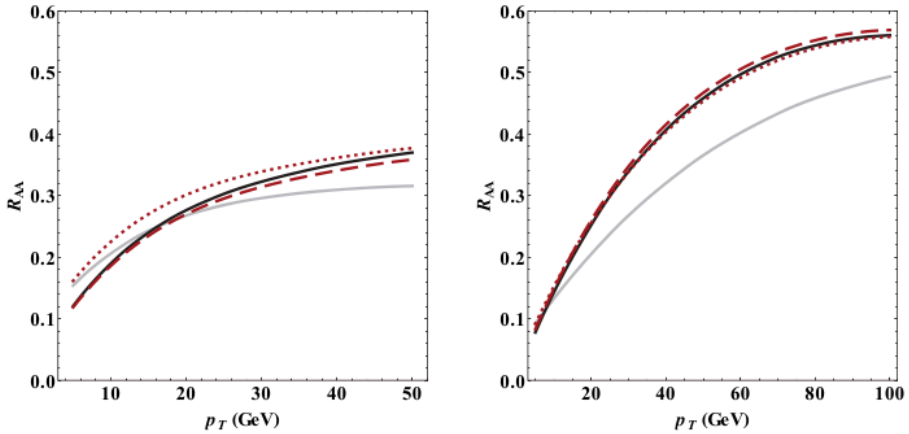

Figure 1. Fixed and running coupling pion R_{AA} results are compared side to side at RHIC (*left*) and LHC (*right*) in CUJET with Glauber static transverse plus Bjorken longitudinal expanding background. The gray opaque curves use a fixed coupling with $\alpha_s = 0.3$, while the black curves use a running coupling with $\alpha_{\max} = 0.4$. The difference is notable, especially in the higher energy range available at the LHC, while RHIC results are left almost unchanged. The sensitivity to the variation of running scales Q_i (cf. eq. (2.1) and following) is measured by the red curves: on one side we decrease the value of all scales Q_i by 50% and lower $\alpha_{\max}$ to 0.3 (red dashed), on the other we increase all scales Q_i by 25% and increase at the same time $\alpha_{\max}$ to 0.6 (red dotted). $\alpha_{\max}$ is constrained to fit $R_{AA}^{\pi,LHC}(p_T \approx 30\ \text{GeV}) = 0.35$.

❖ Uncertainties in running scales

❖ Which running scale dominates?

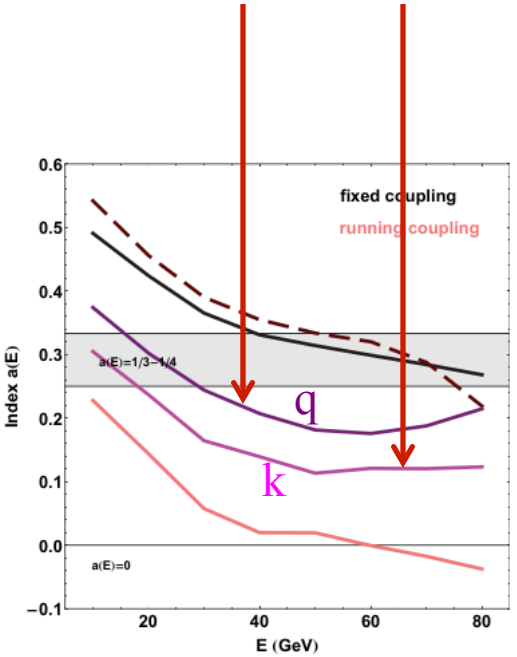

Figure 2. Energy loss index $a(E)$ (cf. eq. (2.9)) for different assumptions of the running coupling in CUJET: fixed effective $\alpha_s = 0.3$ (black), only thermal coupling running (dashed red), only $\alpha_s^2(\mathbf{q}^2)$ running (purple), only $\alpha_s^2(\mathbf{k}^2/(x(1-x)))$ running (magenta), all couplings running (pink). The saturated $\alpha_{\max}$ value is chosen to be equal to 0.4, which corresponds to approximately $Q_0 \sim 1\,\text{GeV}$. The plot shows the energy loss of a light quark ($M = 0.2\,\text{GeV}$) traveling from the origin of the transverse plane and through a gluonic plasma ($n_f = 0$) of size $L = 5\,\text{fm}$, whose density profile is generated from Glauber model and resembles the medium created in a Pb+Pb $\sqrt{s_{NN}} = 2.76\,\text{TeV}$ $b = 0\,\text{fm}$ collision.

Crossing

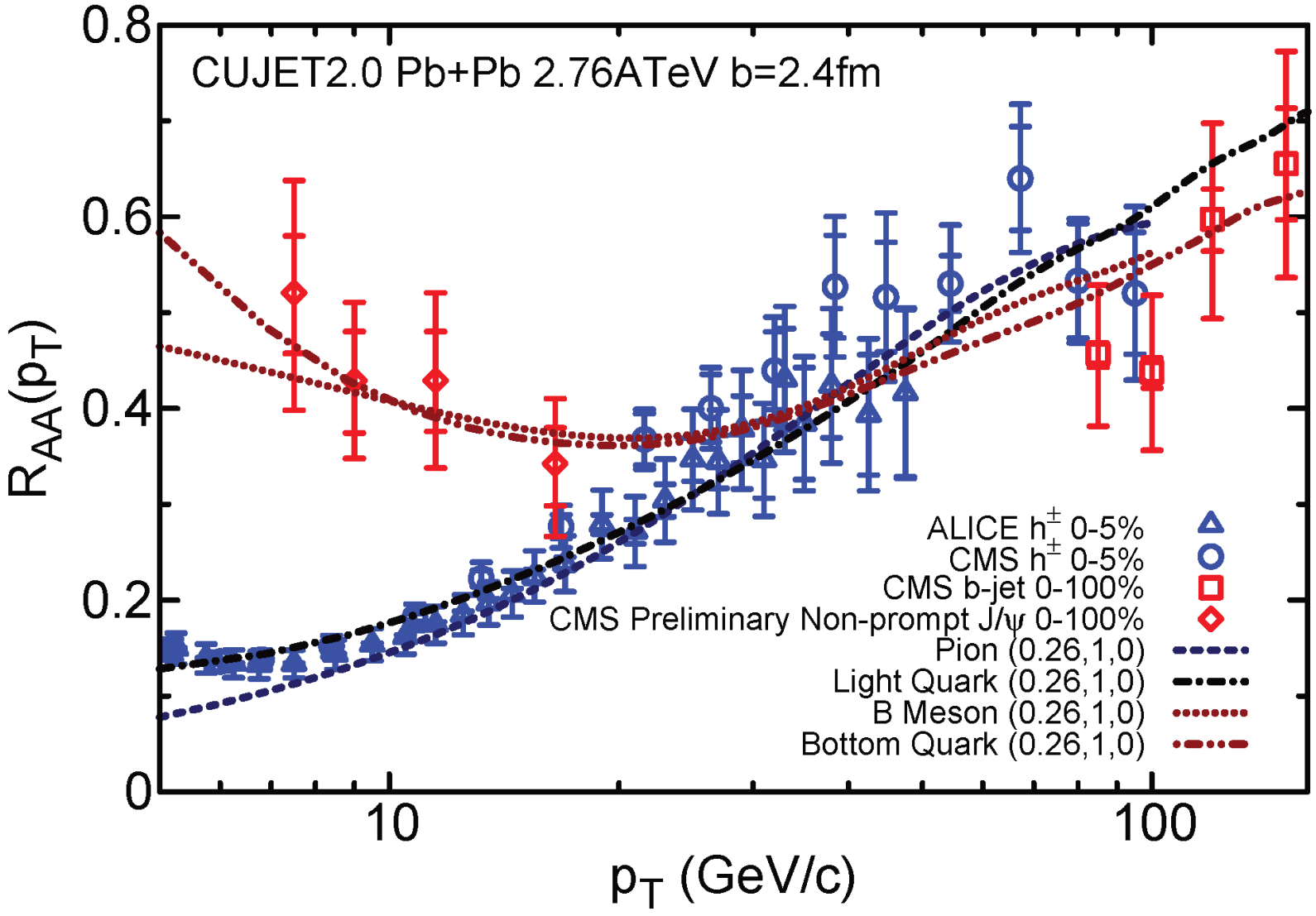
CUJET2.0 Pb+Pb 2.76ATeV b=2.4fm
$R_{AA}(p_T)$
p_T (GeV/c)
0.8
0.6
0.4
0.2
0
10
100
ALICE $h^{\pm}$ 0-5%
CMS $h^{\pm}$ 0-5%
CMS b-jet 0-100%
CMS Preliminary Non-prompt J/ψ 0-100%
Pion (0.26,1,0)
Light Quark (0.26,1,0)
B Meson (0.26,1,0)
Bottom Quark (0.26,1,0)

Similarity between light quark and pion RAA at RHIC and LHC

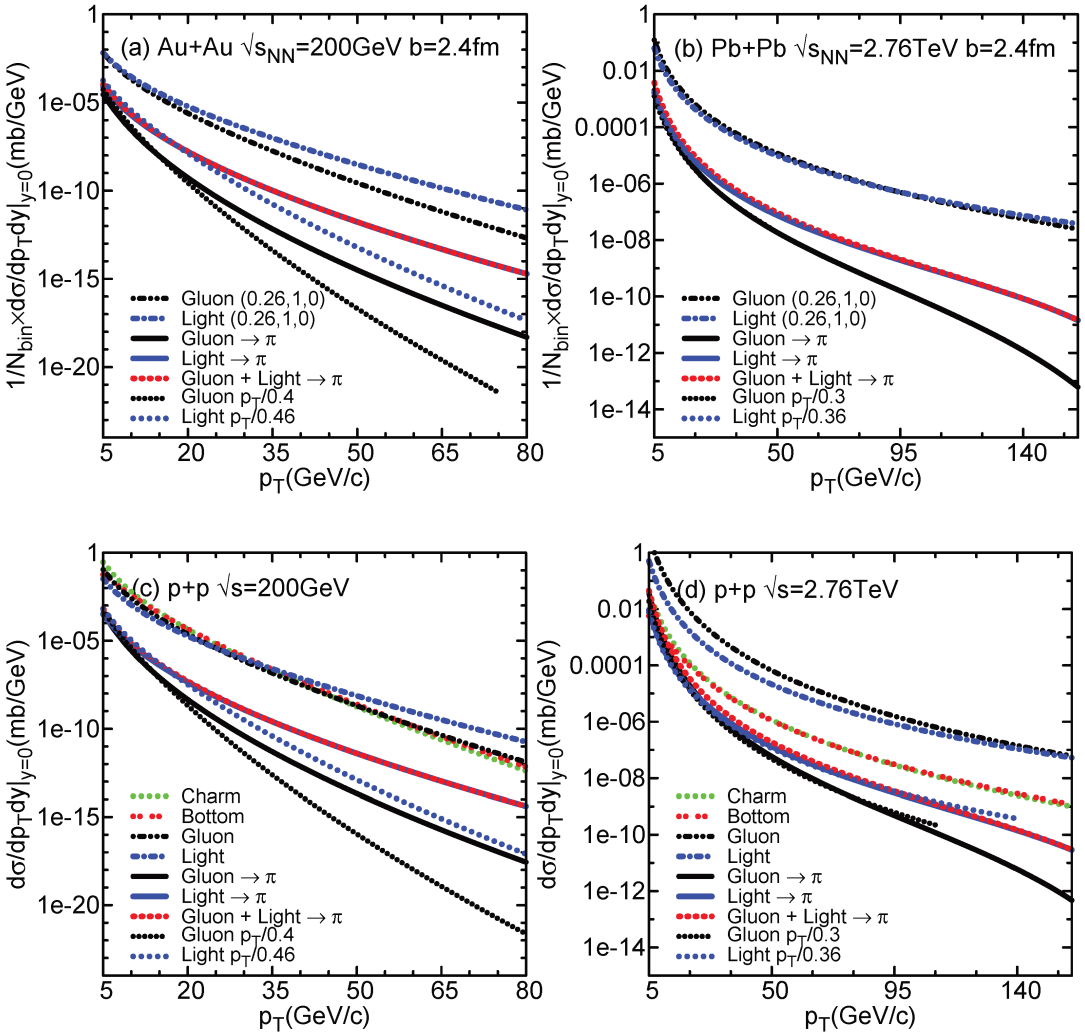

- Larger Casimir for gluon (C_R=3) than quark (C_R=4/3) leads to more energy loss for the gluon, brings their AA production spectra at LHC to the same level
- Different fragmentation ratios of gluon and quark to pion make the light quark's contribution to pion AA spectrum dominant

CUJET: open heavy flavor high pT v2

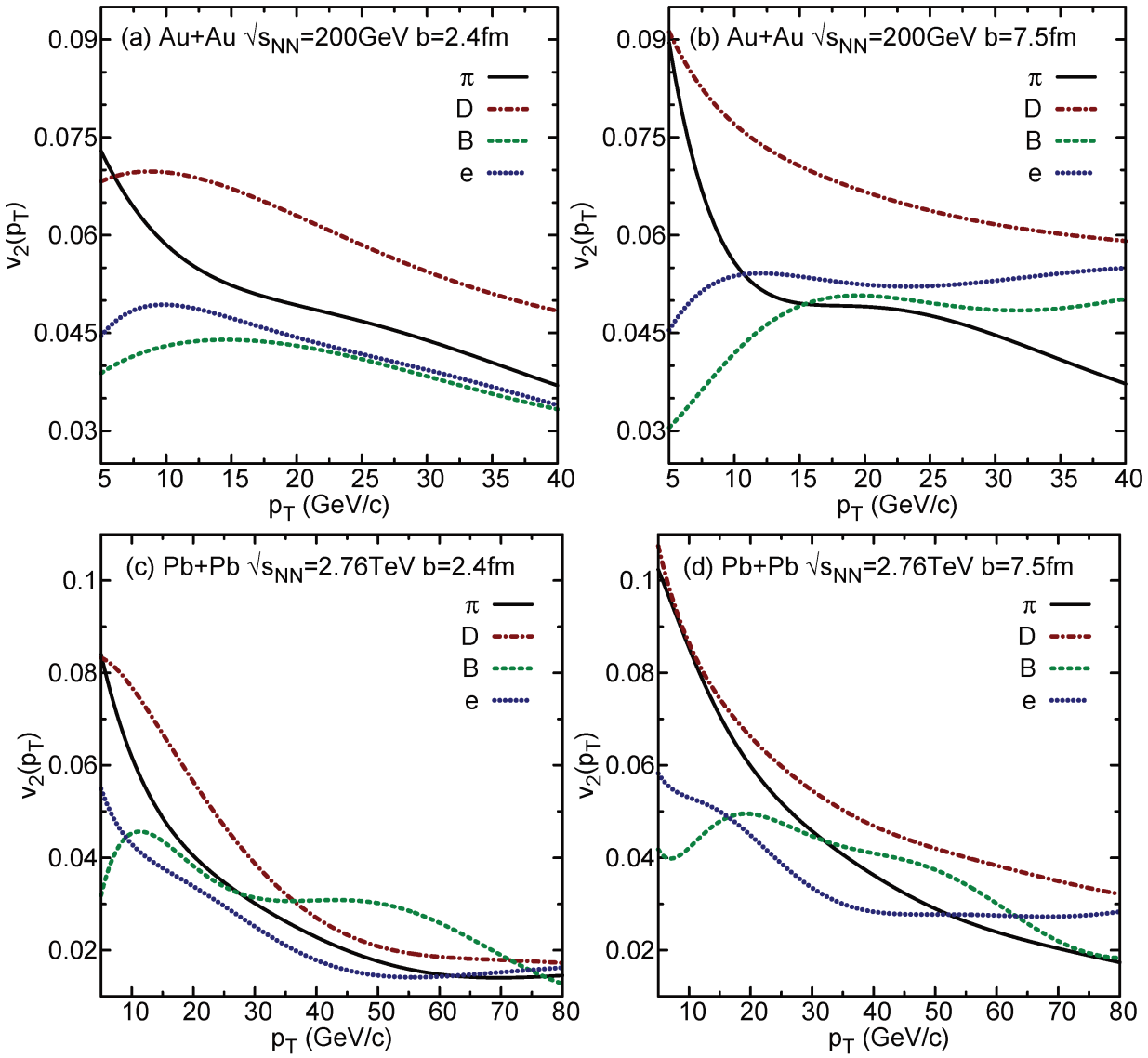

- B meson v2 has a peak at pT~10GeV @ b=2.4fm and pT~20GeV @ b=7.5fm at both RHIC and LHC
- Semi-ordering of the position of the peak for different flavors v2

More on the Polyakov Loop

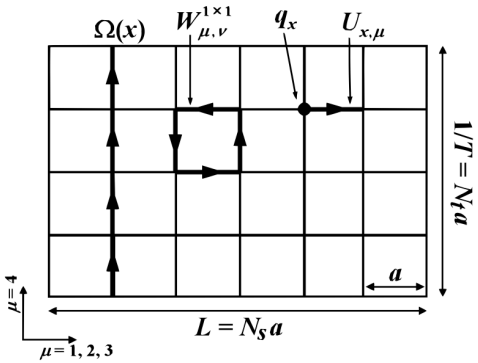

$$U_{x,\mu} = \mathcal{P}\exp\left[ig\int_x^{x+\hat{\mu}} dx_\mu A_\mu(x)\right]$$

$$W^{1\times1}_{\mu\nu}(x) \equiv U_{x,\mu}U_{x+\hat{\mu},\nu}U^\dagger_{x+\hat{\nu},\mu}U^\dagger_{x,\nu}.$$

$$L(\mathbf{x}) = \frac{1}{N_c}\mathrm{tr}\mathcal{P}\exp\left[ig\int_0^{1/T} A_4(\tau,\mathbf{x})d\tau\right] \equiv \frac{1}{N_c}\mathrm{tr}\Omega(\mathbf{x})$$

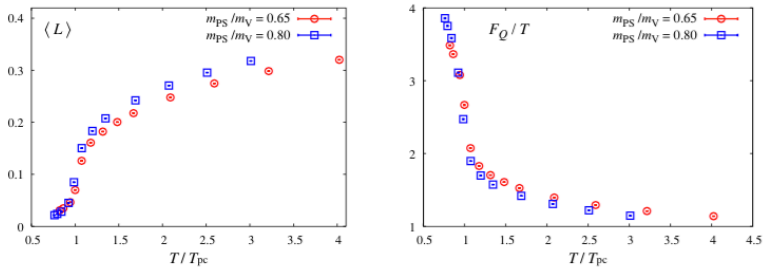

Figure 2.5: Polyakov loop (left) and single-quark free energy (right) on lines of constant physics at $m_{PS}/m_V = 0.65$ (circle) and 0.80 (square) as a function of temperature.

shows the free energy of a single quark defined as

$$\frac{F_Q}{T} = -\ln\langle L\rangle. \tag{2.62}$$

We find that the free energy for smaller quark mass is smaller below T_{pc}, whereas it is larger above T_{pc} than that for larger quark mass. This implies that the anti-screening (screening) properties in the confinement (deconfinement) phase becomes strong when the quark mass is reduced.

The physical meanings of the Polyakov loop can be seen as follows. Consider the equation of motion for the heavy quark field which is written as $e^{-m_Q\tau}\psi$ (upper component of the Dirac spinor). The static Dirac equation for ψ is given as,

$$\left(i\frac{\partial}{\partial\tau} + gA_4(\tau,\mathbf{x})\right)\psi(\tau,\mathbf{x}) = 0. \tag{2.58}$$

The solution is

$$\psi^a(\tau,\mathbf{x}) = \Omega^{ab}(\mathbf{x})\,\psi^b(0,\mathbf{x}), \tag{2.59}$$

where color indices are written explicitly. When the heavy (static) quark is placed at a spatial point $\mathbf{x}$, the partition function (Z_Q) for the single quark can be written by the total Hamiltonian H_Q as:

$$\begin{aligned} Z_Q/Z &= e^{-(F_Q(T,V)-F(T,V))/T} \\ &= \frac{1}{Z}\frac{1}{N_c}\sum_{a=1}^{N_c}\sum_n \langle n|\psi^a(0,\mathbf{x})e^{-H_Q/T}\psi^{\dagger a}(0,\mathbf{x})|n\rangle \\ &= \frac{1}{Z}\frac{1}{N_c}\sum_{a=1}^{N_c}\sum_n \langle n|e^{-H_Q/T}\psi^a(1/T,\mathbf{x})\psi^{\dagger a}(0,\mathbf{x})|n\rangle \\ &= \frac{1}{Z}\frac{1}{N_c}\mathrm{tr}\left[e^{-H/T}\mathrm{tr}\Omega(\mathbf{x})\right] = \langle L(\mathbf{x})\rangle, \end{aligned} \tag{2.60}$$

where F_Q (F) is the free energy with (without) the heavy quark. In the $N_f = 0$ case, the free energy of a single quark can strictly distinguish the confinement phase and the deconfinement phase. Although the Polyakov loop is no longer the order parameter for confinement-deconfinement transition in the case with dynamical quarks, we can utilize the $\langle L\rangle$ as an indicator to separate the cold and hot phases in the parameter space (see Fig. 2.2). The nu-

as the Polyakov loop averaged over all thermal states and spatial points,

$$\langle L\rangle = \frac{1}{Z}\frac{1}{N_s^3}\sum_{\mathbf{x}}\mathrm{Tr}\left[e^{-H/T}L(\mathbf{x})\right]. \tag{2.61}$$

The Polyakov loop has finite values even below T_{pc} because a single heavy quark can exist in the confinement phase due to the dynamical screening from the light quarks. Figure 2.5(right)

Adapted from Maezawa 2007

aE vs aM

Let us focus on the scattering rate from color-electric Coulomb scattering centers experienced by jet partons in

CUJET2.0

$$x\frac{dN}{dx} \propto \ldots \int_{q^2} \left[\frac{n\,\alpha_s^2(q^2)\,f_E^2}{q^2(q^2+f_E^2\mu^2)}\right] \ldots$$

HTL QGP screened
Color electric scatt

With the presence of both electric and magnetic components, the above integrand needs to be generalized as:

CUJET3.0

$$\left[\frac{n_e\left(\alpha_s(q^2)\alpha_s(q^2)\right)f_E^2}{q^2(q^2+f_E^2\mu^2)} + \frac{n_m\left(\alpha^e(q^2)\alpha^m(q^2)\right)f_M^2}{q^2(q^2+f_M^2\mu^2)}\right] \quad (3)$$

Jet + Semi-QGP screened
Color electric scatt

<<

Jet+ Monopole gas
Color magnetic scatt

$$\frac{\alpha_e}{\alpha_m} \sim \alpha_e^2 \sim \frac{1}{10}$$

J.Xu, J.Liao, M.G: arXiv:1411.3673 [hep-ph]

CUJET3.0: v2 and naïve qhat

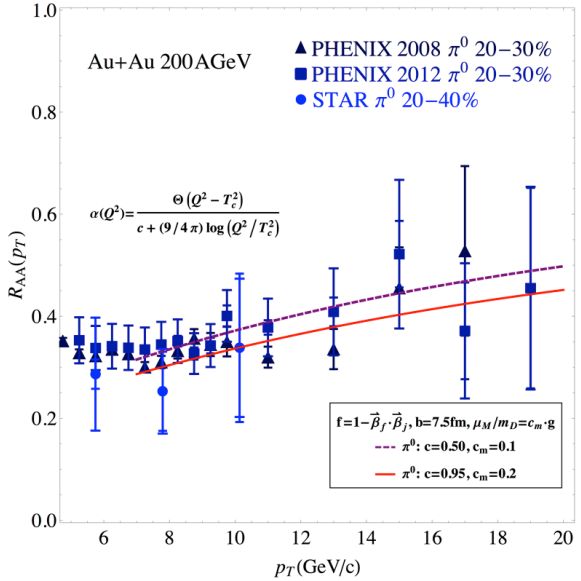

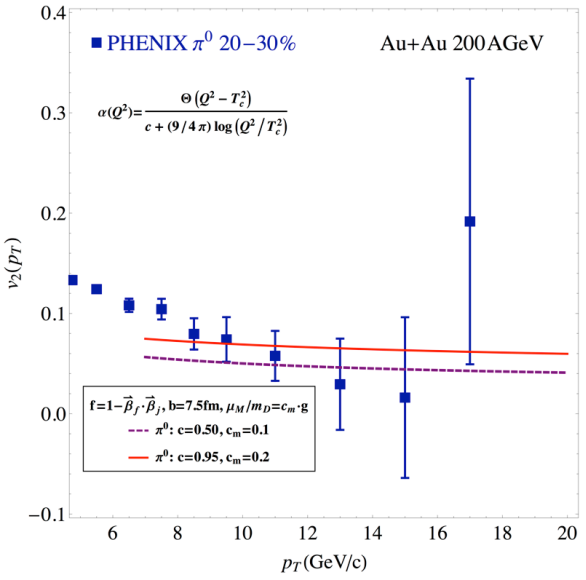

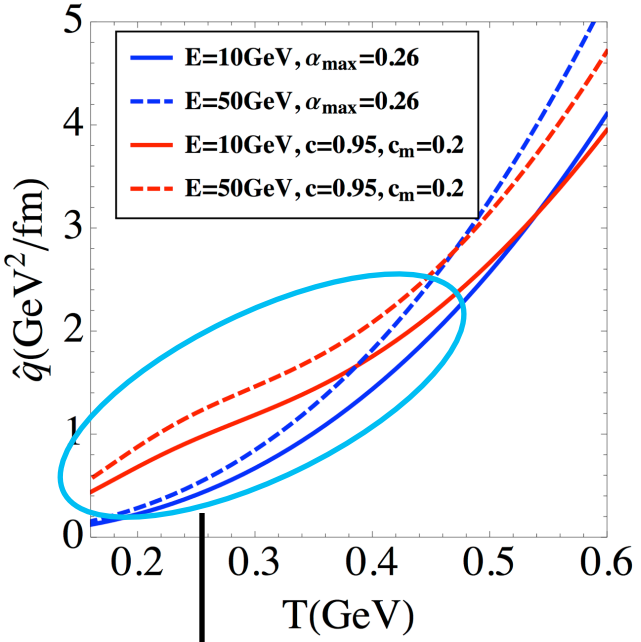

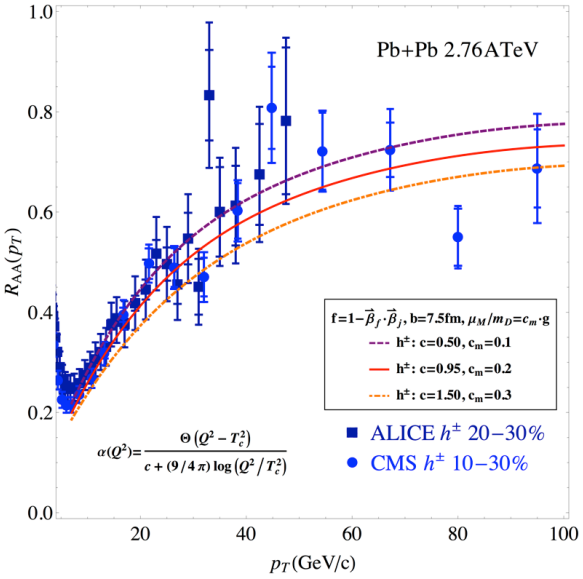

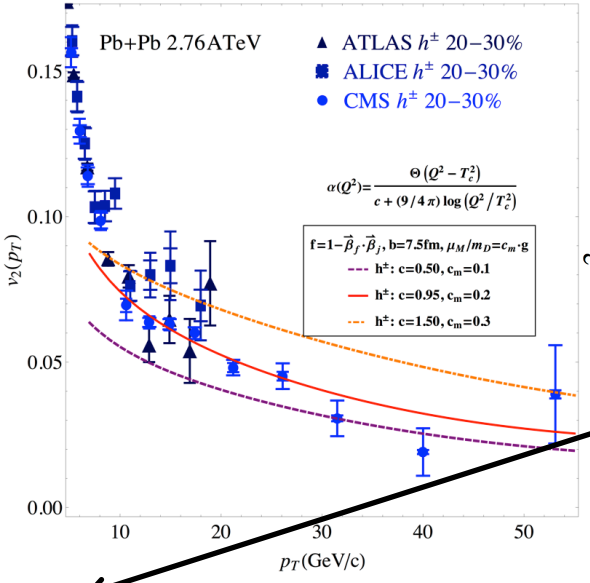

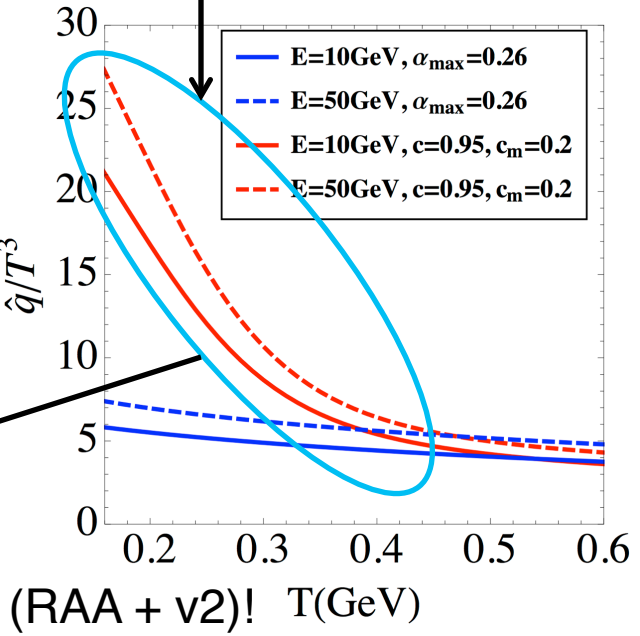

❖ The "volcano" fits (RHIC + LHC) & (RAA + v2)!

CUJET3.0: naïve qhat inversion

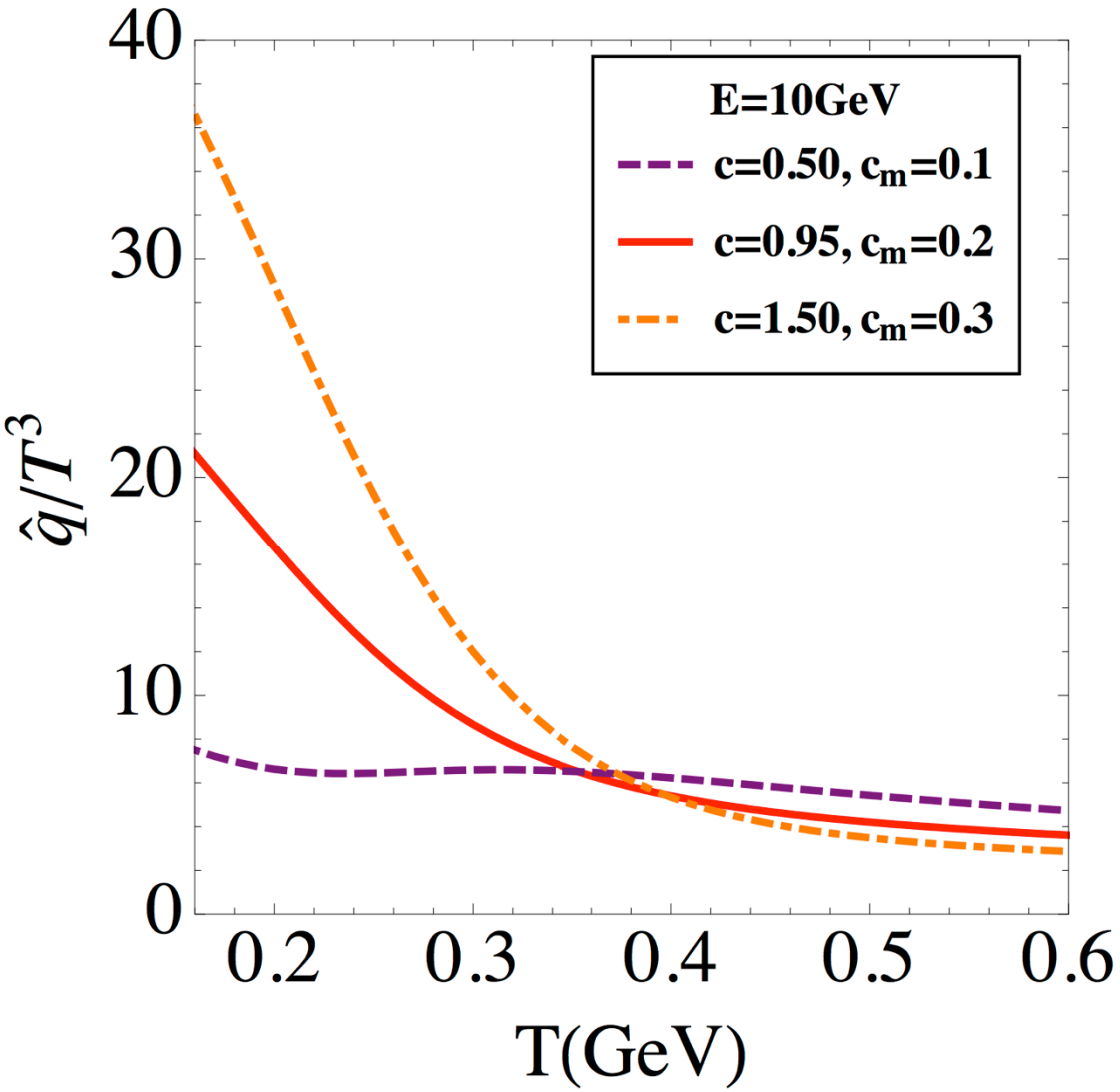

CUJET3.0 = CUJET2.0 + semi-QGP + mag. monopoles

$$\frac{dE}{dx} \propto \ldots \int_{q^2} \left[\frac{n_e \left(\alpha_s(q^2)\alpha_s(q^2)\right) f_E^2}{q^2(q^2+f_E^2\mu^2)} + \frac{n_m \left(\alpha_s^e(q^2)\alpha^m(q^2)\right) f_M^2}{q^2(q^2+f_M^2\mu^2)} \right] \ldots$$

$$\frac{dE}{dx} \propto \ldots \int_{q^2} \frac{n_e\, \alpha_s^2(q^2)\, f_E^2}{q^2(q^2+f_E^2\mu^2)} \ldots$$

$$\frac{dE}{dx} \propto \ldots \int_{q^2} \frac{n_T}{(q^2+f_E^2\mu^2)(q^2+f_M^2\mu^2)} \times \kappa(q^2,T)$$

$$\kappa(q^2,T) \equiv \alpha_s^2(q^2)\,\chi_T \left(f_E^2 + \frac{f_E^2 f_M^2 \mu^2}{q^2}\right) + (1-\chi_T)\left(f_M^2 + \frac{f_E^2 f_M^2 \mu^2}{q^2}\right)$$

$$\chi_T = c_q\, L + c_g\, L^2 \qquad L(\mathbf{x}) = \frac{1}{N_c}\mathrm{tr}\mathcal{P}\exp\left[ig\int_0^{1/T} A_4(\tau,\mathbf{x})d\tau\right]$$

$$f_E = \sqrt{\chi_T}$$

$$f_M = C_m\, g_T$$

$$x_E \frac{dN_g^{n=1}}{dx_E} = \frac{18C_R}{\pi^2}\frac{4+N_f}{16+9N_f}\int d\tau\, n(\mathbf{z})\Gamma(\mathbf{z}) \int d^2k$$
$$\times\, \alpha_s\left(\frac{\mathbf{k}^2}{x_+(1-x_+)}\right) \int d^2q \frac{\alpha_s^2(\mathbf{q}^2)}{\mu^2(\mathbf{z})} \frac{f_E^2\mu^2(\mathbf{z})}{\mathbf{q}^2(\mathbf{q}^2+f_E^2\mu^2(\mathbf{z}))}$$
$$\times \frac{-2(\mathbf{k}-\mathbf{q})}{(\mathbf{k}-\mathbf{q})^2+\chi^2(\mathbf{z})}\left[\frac{\mathbf{k}}{\mathbf{k}^2+\chi^2(\mathbf{z})} - \frac{(\mathbf{k}-\mathbf{q})}{(\mathbf{k}-\mathbf{q})^2+\chi^2(\mathbf{z})}\right]$$
$$\times \left[1-\cos\left(\frac{(\mathbf{k}-\mathbf{q})^2+\chi^2(\mathbf{z})}{2x_+E}\tau\right)\right]\left(\frac{x_E}{x_+}\right)\left|\frac{dx_+}{dx_E}\right| \qquad (1)$$

$$\Gamma(\mathbf{z}) = u_f^\mu n_\mu \qquad n = (1,\vec{\beta}_{jet})$$

Liu et al. 07'; Baier et al. 07' $\qquad u_f^\mu = \gamma_f(1,\vec{\beta}_f)$

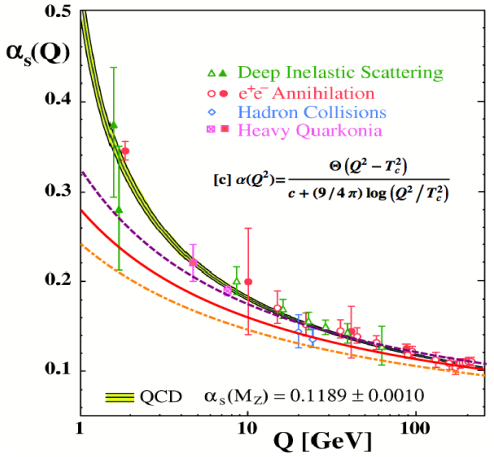

$$\alpha_s^2(q^2) \approx [1/[c+(9/2\pi)Log(q/\Lambda)]]^2$$

CUJET3.0: RAA at RHIC & LHC

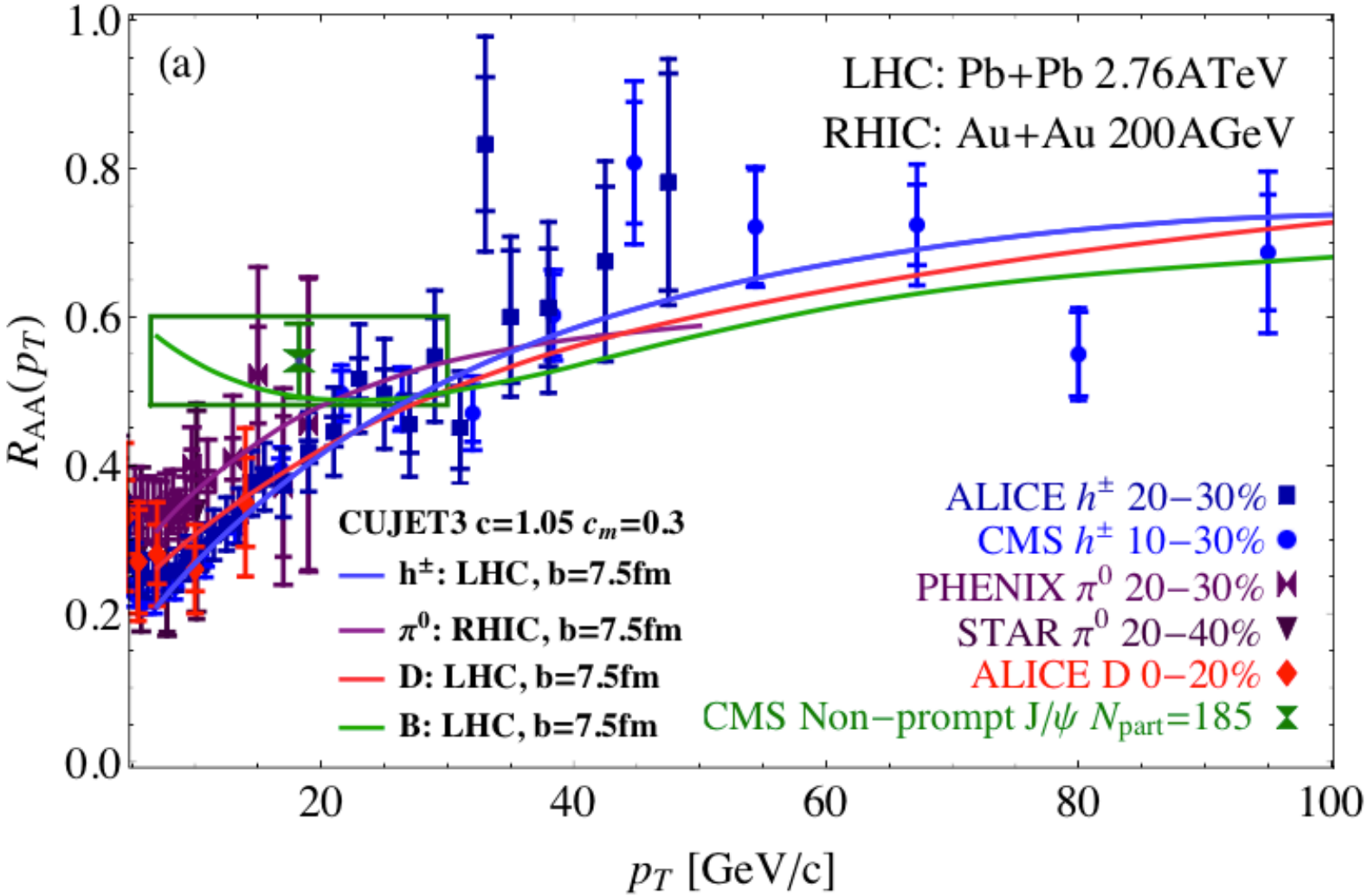

$$R^h_{AA}(p_T, y; \sqrt{s}, b) = \frac{dN^h_{AA}/dydp_T}{N_{\rm bin}\, dN^h_{pp}/dydp_T}.$$

- CUJET3.0 with (c,c_m)=(1.05,0.3) fits R_{AA} at both RHIC and LHC

CUJET3.0: v2 at RHIC & LHC

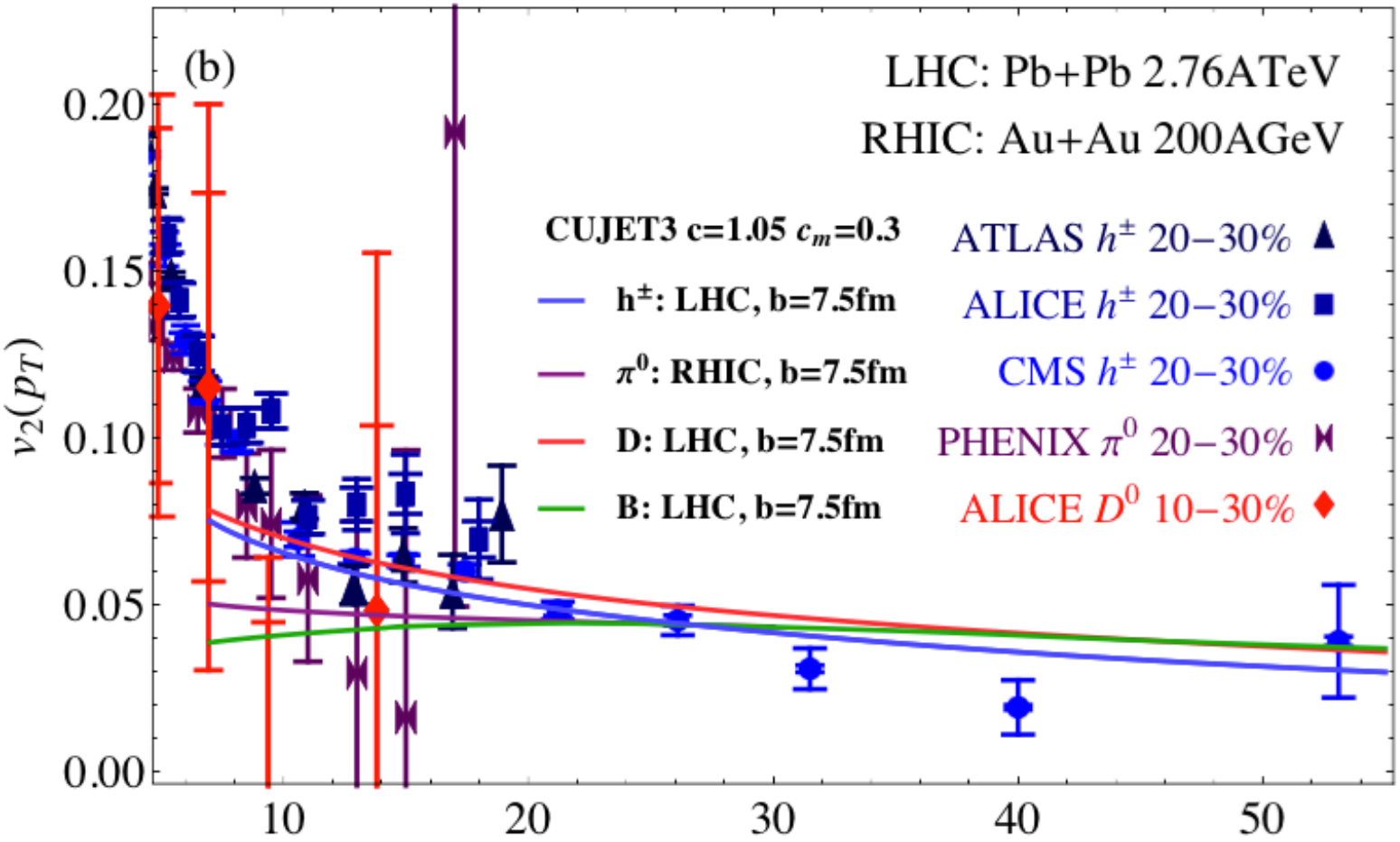

$$\frac{dN^h}{dy p_T dp_T d\phi}(p_T,\phi,y;\sqrt{s},b) = \frac{1}{2\pi}\frac{dN^h}{dy p_T dp_T}(p_T,y) \times \left[1+2\sum_{n=1}^{\infty} v_n^h(p_T,y)\cos\left(n(\phi-\Psi_n^h)\right)\right] . \qquad (11)$$

- CUJET3.0 with (c,c_m)=(1.05,0.3) fits v_2 at both RHIC and LHC simultaneously

Fast Liberation Scheme (FL)

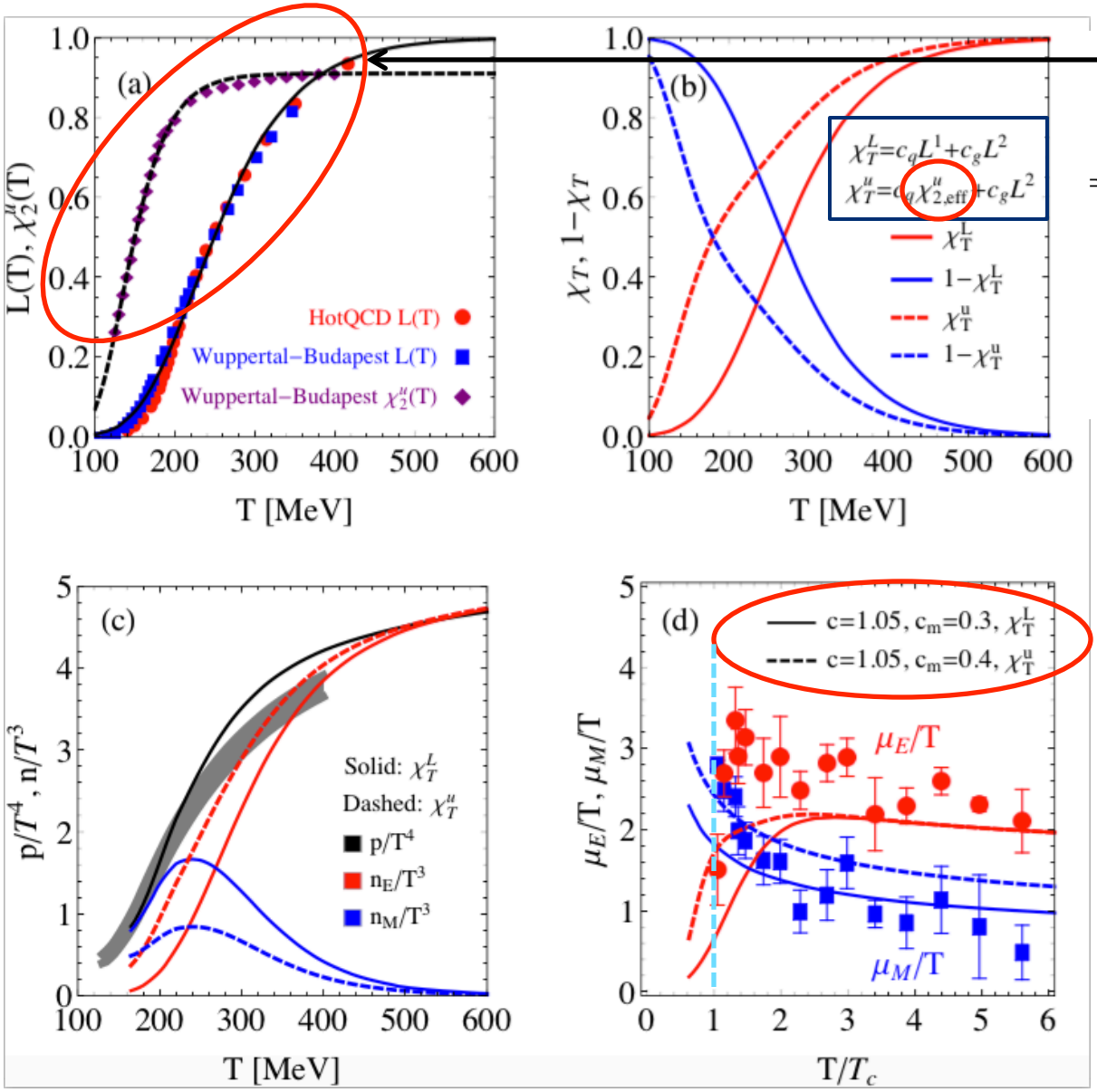

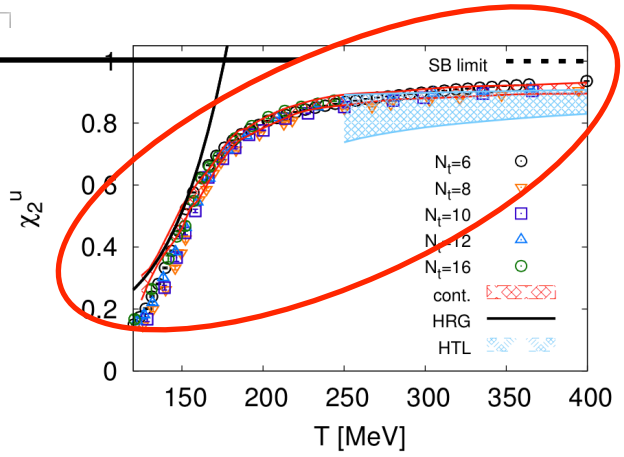

Wuppertal-Budapest JHEP 1201 (2012) 138

- Fast Quark Liberation: Fit to lattice QCD u quark number susceptibility
- Note the shift of E&M fractions and screening masses near Tc

$$\frac{p}{T^4} = \frac{1}{VT^3} \ln Z(V, T, \mu_B, \mu_S, \mu_Q)$$

$$\chi_{lmn}^{BSQ} = \frac{\partial^{l+m+n} p/T^4}{\partial(\mu_B/T)^l \partial(\mu_S/T)^m \partial(\mu_Q/T)^n}.$$

$$\chi_2^X = \frac{1}{VT^3} \langle N_X^2 \rangle$$

CUJET3.0: RAA & v2 at RHIC & LHC in FL

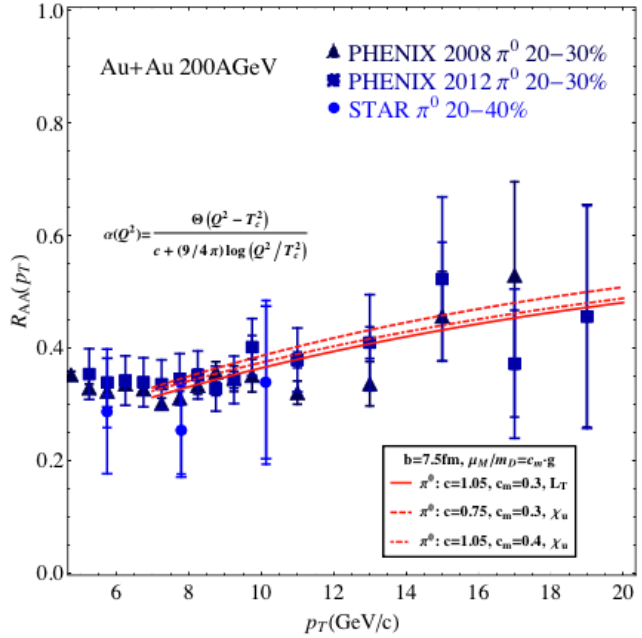

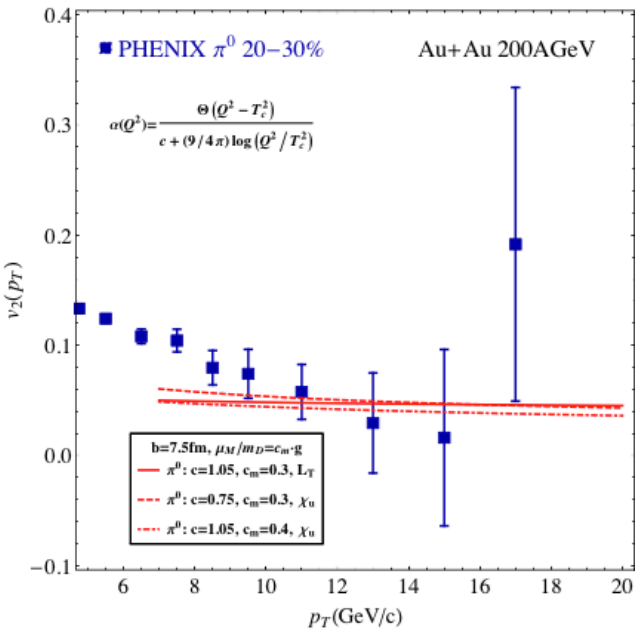

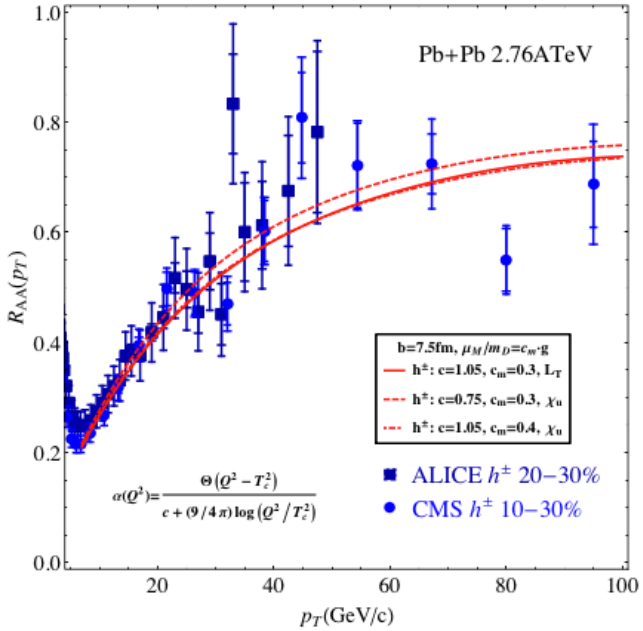

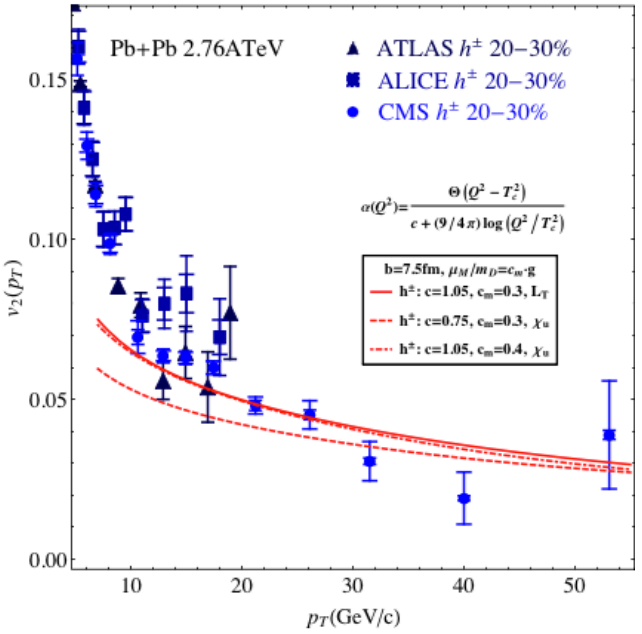

CUJET3.0: RAA & v2 at RHIC & LHC in FL

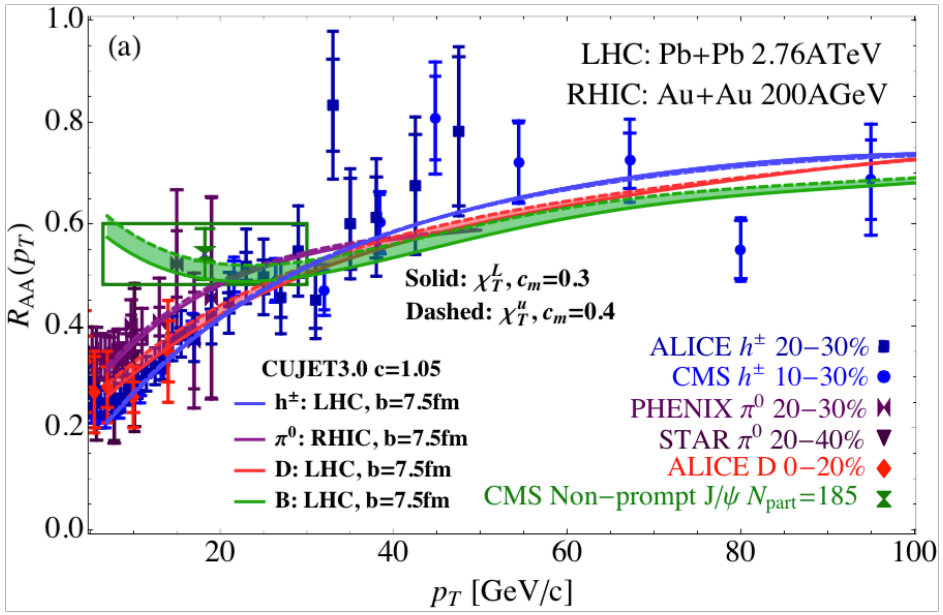

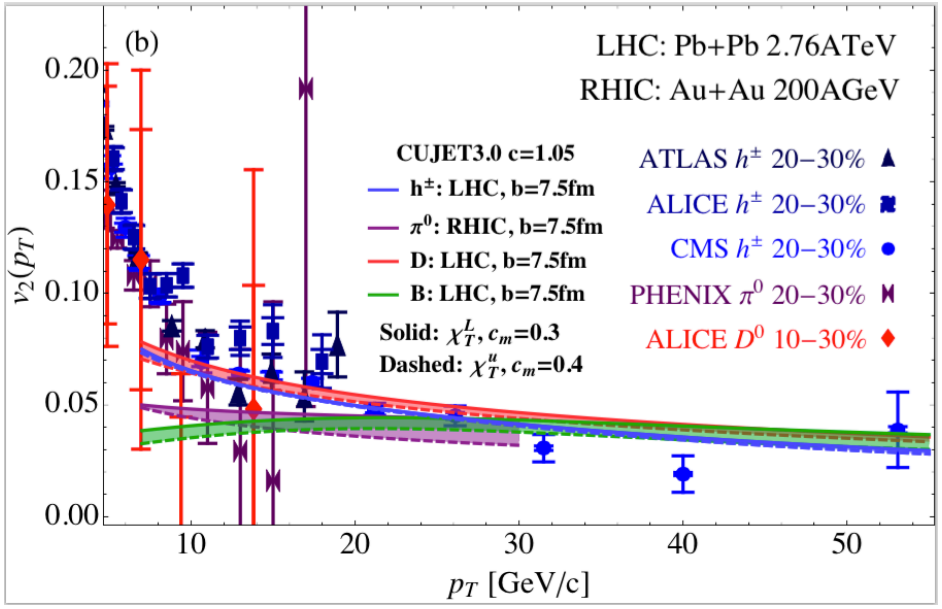

- In the fast liberation scheme, the CUJET3.0 model with $(c,c_m)=(1.05,0.4)$ fits both R_{AA} and v_2 at both RHIC and LHC